

Task C
Electroweak Interactions at BaBar, ILC, and CMS
University of Wisconsin

DOE Award #DE-FG02-95ER40896

R. Prepost – Principal Investigator
S. Dasu – Principal Investigator

Draft 5/7/08, V 1.0

1 PROJECT OVERVIEW

The study of weak and electromagnetic interactions has been the prime focus of research under this task starting with photo-production experiments at SLAC in the 70s through the current R&D project for building a linear collider (ILC) to make precision measurements of electro-weak symmetry breaking phenomena.

The major group effort continues to be analysis and support activities with the BaBar detector at PEP II. For the past several years there has also been a commitment to R&D for the International Linear Collider (ILC) and as the PEP II/BaBar program comes to an end, more of the group effort will be directed toward the ILC. R. Prepost continues a long term program for the development and design of the ILC polarized source and H. Band has taken on the responsibility as a Working Group leader for the muon system in the silicon detector (SiD) design concept. These activities are described more fully in subsequent sections.

The long term nature of the ILC program makes it unsuitable for postdoctoral researchers on a full time basis. In order to provide both detector development and physics analysis opportunities for the postdocs, we are linking this task through S. Dasu to the CMS experiment, which will begin data taking as BaBar shuts down.

2 TECHNICAL PROGRESS

2.1 BaBar Overview

Our group had a productive year completing several analyses and giving conference talks. K. Flood's talks on the discovery of mixing of charm mesons were a highlight at the Spring 07 Moriond Conferences. In addition to leading an analysis group on BaBar, M. Pierini has been active in the Unitarity Triangle Fit group. C. Vuosalo, K. Flood and H. Band further improved Babar muon identification using new statistical pattern recognition techniques.

Several group members are in BaBar leadership roles. K. Flood served as co-convenor of the Particle Identification Group (PID) in 2006. M. Pierini is co-convenor of the Two-Body Charmless B Decay Analysis Group and H. Band has served as System Manager of the IFR-RPC detector system since 2001.

Senior members of the group are involved in physics analysis review, and supervision of student and postdoctoral research. J. Hollar (2006) and A. Eichenbaum (2004) have graduated with their theses written under the supervision of Prof. Prepost. P. Tan (2005) obtained his thesis under the supervision of Prof. Dasu, and C. Vuosalo began his thesis work in 2006.

Postdoctoral researcher Dr. F. Di Lodovico (2001-2005) moved on with a faculty position at the Queen Mary College, London, while Dr. A. Mohapatra (2001-2005) moved on to a physics/computing researcher position in the Wisconsin CMS group. M. Pierini has been awarded a prestigious CERN fellowship.

2.2 BaBar Detector Support Activities

2.2.1 Instrumented Flux Return Endcap

The Instrumented Flux Return (IFR) detector system consists of Resistive Plate Chambers(RPCs) inserted into the gaps of the Endcap flux return steel. The barrel part of the IFR is instrumented with Limited Streamer Tubes(LST).

BaBar was the first experiment to use bakelite RPCs as a main detector in a colliding beam experiment. Unfortunately, the original bakelite RPCs in BaBar experienced many problems due to a variety of causes (excessive linseed oil, poor quality control, aging of the graphite coating, and gas leaks) which lead to steadily decreasing RPC efficiencies. The barrel RPCs were replaced by LST chambers in stages in 2004 and 2006. The RPCs in the forward endcap were replaced in 2002 as part of an upgrade lead by H. Band and F. Ferroni (Roma), which also increased the amount of absorber in the forward region. The new RPCs were built under a stringent Quality Assurance program developed by the IFR group. Many of these QA improvements have been adopted by the LHC detectors (CMS and ATLAS). The performance and aging of these new BaBar RPCs is thus of special interest to the worldwide RPC community. The upgrade and aging studies have been documented in three NIM publications in 05, and talks by H. Band at IEEE03, IEEE04, RPC2005 and IEEE06.

Over 40% of the BaBar muon acceptance is covered by the RPC Endcaps with greater than 36% of the acceptance in the forward endcap. Although the new forward RPCs have performed well (the average RPC efficiency has decreased slowly from 93% in 02 to 90% in 07), more than routine maintenance has been required to keep the RPCs efficient. Background rates in the outermost forward layers have risen as the machine luminosity has increased, preventing normal chamber operation. The Wisconsin group led the design and installation of a shielding wall significantly reducing backgrounds. All outer layer RPCs have been on since the start of Run 5. The efficiency of these outermost layers was initially disappointing. Measurements showed that the input gas was preferentially drying the Bakelite near the gas inlets leading to an increase in the Bakelite bulk resistivity. At moderate background rates the increased resistance lowered the chamber efficiency. A system, built by H. Band, to add water to the input gas stream was installed and after several months of humidified gas the efficiency was completely restored. The outer layers have since performed reliably although further shielding may be required if the luminosity doubles as planned. The additional information from these outer layers has improved the performance of the muon selectors as seen in Fig. 1.

The Forward RPCs have experienced widely different background and luminosity-driven singles rates ($0.01 - 20 \text{ Hz/cm}^2$) depending on position within the endcap. The highest rates are centered around the beamline in the inner layers. The projected integrated charge in the high rate regions exceeded the thresholds for damage to the RPC graphite layers. One way to lower the amount of charge per track hit is to convert the RPCs from streamer mode to saturated avalanche mode operation as used in the LHC RPCs. However, avalanche mode electronic signals are much smaller than streamer and require preamplification. In collaboration with C. Lu of Princeton and A. Cotta-Ramusino of Ferrara, 2 generations of amplifiers on several RPC chambers have been tested on RPC chambers in avalanche mode. Tests to date are very encouraging. RPC currents have been reduced by 1/4 and efficiencies at small radii were restored. Consequently, the highest rate RPCs are currently being converted to avalanche mode.

2.2.2 BaBar Muon Identification

Members of the Wisconsin group (A. Mohapatra, J. Hollar, K Flood, and H. Band) developed and maintained a neural net (NN) muon identification algorithm that has become the BaBar standard, replacing previous cut based and likelihood identifiers. A plot of the NN performance between 2000 and 2005 is shown in Fig. 1. The NN algorithm has a higher efficiency at fixed pion rejection rates than the cut-based algorithm. Also evident are the performance improvements from the endcap upgrade and shielding wall installation. The use of present NN muon selector increases the relative efficiency for di-muon signal in the $B \rightarrow K^* l^+ l^-$ analysis by 30% with no increase in hadronic backgrounds.

K. Flood and C. Vuosalo have explored new methods beyond neural networks for optimizing muon identification. The most promising of these are *boosted decision trees* (BDT), which allow seamless integration of measurements from all detector systems in a single algorithmic framework. Unlike neural networks, the performance of decision trees is robust in the presence of incomplete data, improving the selector performance in the BaBar barrel during Runs 2-5 when many of the original RPCs were inefficient. A study of possible detector variables and implementations has lead to a new BDT muon selector whose performance is shown in Fig. 1b. This selector will be available to BaBar analyses by summer 07.

2.3 BaBar Physics Analysis

After discovering CP violation phenomena in the B meson sector, the BaBar physics program has moved on to firmly establish the CKM quark mixing formalism in the Standard Model (SM). A global analysis of the B physics data is now providing very tight constraints on physics beyond the Standard Model. Our group is not only continuing to make several important measurements using BaBar data, but has also emerged as a leader in the interpretation and phenomenological analysis of the flavor physics data. Keeping with the tradition of our group interests, we have concentrated on studying electro-weak penguin contributions to the B meson decays ($b \rightarrow s\gamma$, $b \rightarrow s\ell\ell$ and now $b \rightarrow s\nu\nu$). We have also broadened our analysis efforts in 2005 to cover the study of the CP asymmetry in QCD penguin induced B -meson decays (Pierini), and $D^0\bar{D}^0$ mixing (Flood).

Interest in the electro-weak flavor changing neutral currents (FCNC) induced decays of the b quarks, e.g.,

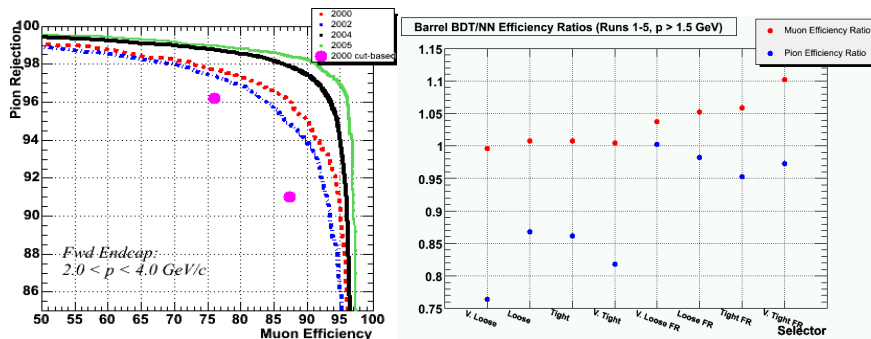


Figure 1: The performance of BaBar neural net and cut-based muon identification algorithms is plotted for several run periods. The higher the pion rejection (in %) at fixed muon efficiency, the better the algorithm. The NN reduced the pion mis-identification in 2000 by a factor of two when compared to the cut-based algorithm. Also evident is the improved performance in 2004 due to the endcap upgrade and the further improvement in 2005 when improved shielding allowed routine use of the outermost RPC layers. b) Relative performance of the BDT muon selector described in the text compared to the NN selectors. At similar muon efficiency the BDT rejects more pions. At similar pion rejection, the BDT accepts more muons.

$b \rightarrow s\gamma$, $b \rightarrow sl^+l^-$ and $b \rightarrow d\gamma$, stems from the fact that FCNC are highly suppressed. In the Standard Model, there are only small higher order contributions to these processes. Any experimental deviations from these predictions can point to new physics signatures. Prior measurements of branching ratios for these decays have already limited new physics contributions severely. However, contributions beyond the Standard Model are often limited by uncertainties in theoretical predictions, especially for the exclusive decays of B mesons, e.g., $B \rightarrow K^*\gamma$. However, measurements of various ratios and asymmetries in these B meson decays and improved inclusive measurements continue to be of interest.

Time dependent CP asymmetries enabled measurement of the angles of the Unitarity triangle. In particular, the golden mode, $b \rightarrow c\bar{c}s$ tree decay, has enabled very accurate measurement of $\sin 2\beta$. Several new modes for the measurement of $\sin 2\beta$ in QCD penguin induced decays have been identified and measured. These loop induced decays can carry subtle effects from new physics contributions which are not present in the golden tree mode. An intriguing discrepancy of only few standard deviations is seen in the comparison of the tree and penguin mode measurements. Our group is working to clarify the present situation by identifying and measuring modes which are less susceptible to theoretical problems.

Our group is also involved in charm mixing analysis. In the Standard Model (SM), $D^0\bar{D}^0$ mixing typically proceeds through box diagram loops and is expected to be much smaller than in the B system. There are many new physics scenarios, which could yield large enhancements to the mixing rate. K. Flood used a fully reconstructed tag technique to place a limit on the D-mixing. He also participated in the review of an analysis which used the full BaBar data set to obtain a 4σ evidence for charm mixing, which he presented at the Spring 07 Moriond conference.

2.3.1 Measurement of the Inclusive Process: $b \rightarrow s\gamma$

Former student A. Eichenbaum (PhD 2004) worked with former Research Associate Dr. F. Di Lodovico on a semi-inclusive measurement of the $b \rightarrow s\gamma$ process. The results using data collected through 2002 for the branching fraction, γ -spectrum and CP asymmetries were published in Pub. 76 and Phys. Rev. Lett. **93**, 021804 (2004). The branching fraction obtained is compared to measurements from other experiments in the Fig. 2. The photon energy spectrum obtained in this analysis and the moments of that spectrum yielded information about the B meson parameters, which were used to reduce the uncertainties in measuring V_{ub} down to the 5% level. The direct CP and isospin violating asymmetry results for this process, shown in

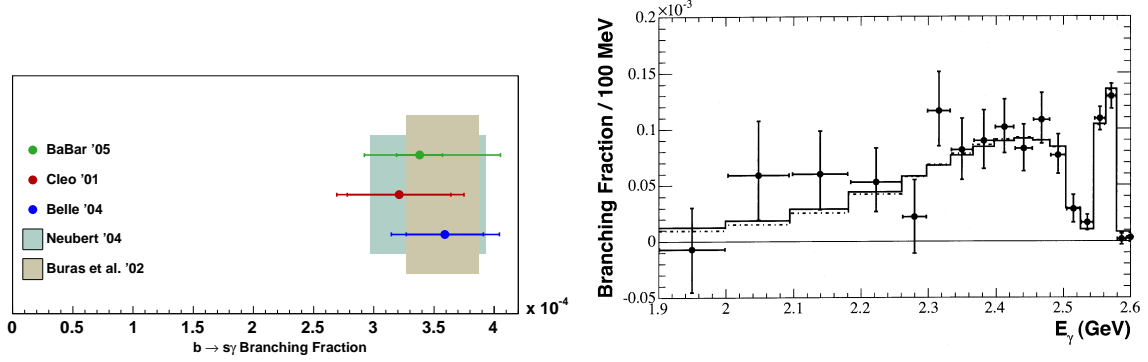


Figure 2: The total branching fraction for fully inclusive $b \rightarrow s\gamma$ process from this measurement (left) and the photon spectrum obtained from the semi-inclusive $b \rightarrow s\gamma$ analysis (right). The sharp peak due to K^* decays is clearly seen.

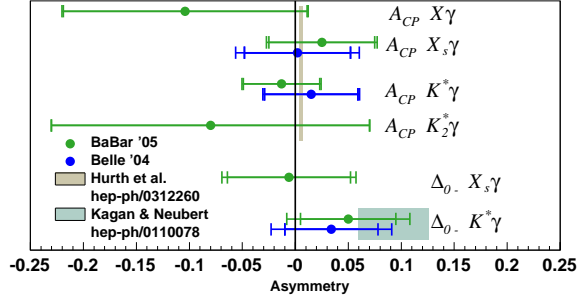


Figure 3: Summary of CP (A_{CP}) and isospin (Δ_{0-}) violating asymmetries measured in semi-inclusive (X_s) and exclusive (K^*) $b \rightarrow s\gamma$ decays. Theoretical uncertainties are indicated by the width of the vertical bands around zero for A_{CP} and around 0.1 for Δ_{0-} .

Fig. 3, are consistent with the Standard Model expectations. However, this result is dominated by statistical errors and will continue to be of interest for new physics searches even with an order of magnitude more data. A. Eichenbaum, under the supervision of R. Prepost, completed his Ph.D. degree in August 2004 with a thesis based on this analysis.

2.3.2 Measurement of $B \rightarrow K^*\gamma$, $B \rightarrow \rho\gamma$, and $B \rightarrow \omega\gamma$

The measurement of $B \rightarrow K^*\gamma$ was carried out using data collected through 2002 by Prof. S. Dasu and former graduate student P. Tan (Ph.D. 2005). The experimental uncertainty on the branching fraction is significantly better than the theoretical uncertainty as shown in Fig. 4(left) (Phys. Rev. D **70**, 112006 (2004)). However, the limits on the CP and isospin violating asymmetries of $B \rightarrow K^*\gamma$ decays, which can constrain certain classes of new physics contributions are interesting in their own right, and are also shown in Fig. 3. These results, which are currently statistically limited, are also consistent with zero in agreement with the SM.

Graduate student P. Tan processed the full BaBar data set collected through 2004, to obtain the limits on the $B \rightarrow \rho\gamma$ and $B \rightarrow \omega\gamma$ branching fractions, which are predicted to be on the order of 10^{-6} as shown in the Fig. 4(right) (Pub. 133). These branching fraction limits and the measured $B \rightarrow K^*\gamma$ values were used to constrain $|V_{td}/V_{ts}|$. P. Tan completed his Ph.D. thesis based on this analysis under the supervision of Prof. Dasu.

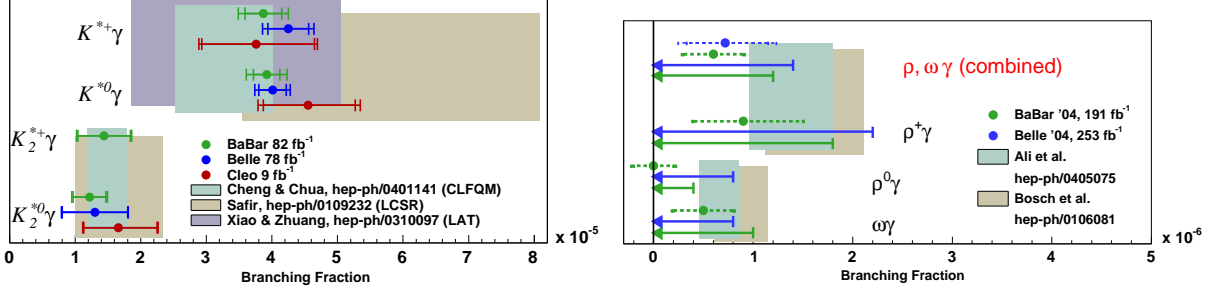


Figure 4: Summary of exclusive $B \rightarrow K^* \gamma$ (left) and exclusive $B \rightarrow \rho \gamma$ and $B \rightarrow \omega \gamma$ (right) branching fraction measurements.

2.3.3 Measurement of $B \rightarrow K^* \ell^+ \ell^-$ and $B \rightarrow K \ell^+ \ell^-$

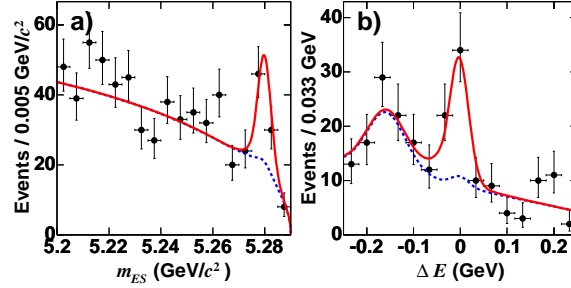


Figure 5: Data fit used to extract $B \rightarrow K \ell^+ \ell^-$ signal projected to (a) the beam energy constrained invariant mass of the reconstructed tracks (M_{ES}) which should peak at m_B , and (b) the difference in energy reconstructed and expected (ΔE), which should peak at 0. The satellite peak at negative ΔE is due to feed-down from $B \rightarrow K^* \ell^+ \ell^-$.

Graduate student J. Hollar (Ph.D. 2006), working under the supervision of Prof. Prepost, measured the exclusive decays $B \rightarrow K \ell^+ \ell^-$ and $B \rightarrow K^* \ell^+ \ell^-$ decays, which provide more observables, such as the K^* polarization and the forward-backward asymmetry of the hadron and lepton. These observables are sensitive to new physics effects that can masquerade in the penguin loops. Hollar's analysis capitalizes on a BaBar champagne award winning neural network based muon selector developed by Hollar and former Research Associate Dr. A. Mohapatra. The projections of the fits used to extract $B \rightarrow K \ell^+ \ell^-$ and $B \rightarrow K^* \ell^+ \ell^-$ signals are shown in the Figs. 5 and 6 respectively. The summary of the branching fractions measured from these signals are compared to those obtained by the Belle collaboration in Fig. 7. There is a small discrepancy between them, which needs to be resolved with additional data.

The forward-backward asymmetry A_{FB} between the lepton and the B -meson flight direction in the dilepton rest frame is of interest. The predictions from models beyond the SM can be significantly different from the SM and can constrain specific terms of the operator product formalism used to make these predictions. A deviation from the SM expectation is also possible in the longitudinal polarization of the K^* . Hollar has published measurements of both these quantities as shown in the Figs. 8 and 9. These measurements, currently limited by statistics, can be improved significantly with additional data to constrain the new physics parameter space. The results based on this analysis have been published in Pub. 55.

2.3.4 Inclusive $b \rightarrow s \ell^+ \ell^-$ analysis

The $K^{(*)} \ell^+ \ell^-$, analysis has been extended by postdoctoral associate K. Flood to include Run 5 data (40% more luminosity), improved muon particle identification ($\sim 20\%$ signal yield increase in all muon modes),

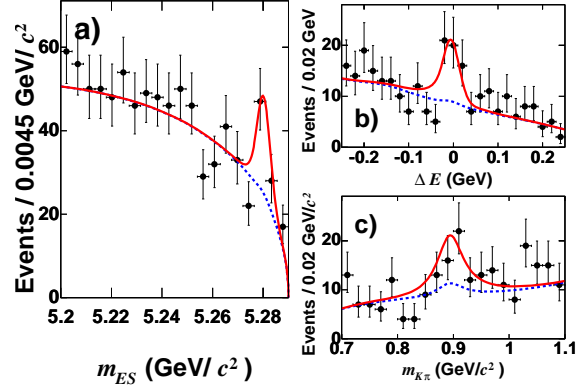


Figure 6: Data fit used to extract $B \rightarrow K^* \ell^+ \ell^-$ signal projected to (a) M_{ES} and (b) (ΔE) is shown. The invariant mass of K, π (c) shows a peak at the m_{K^*} confirming that the signal is that of $B \rightarrow K^* \ell^+ \ell^-$.

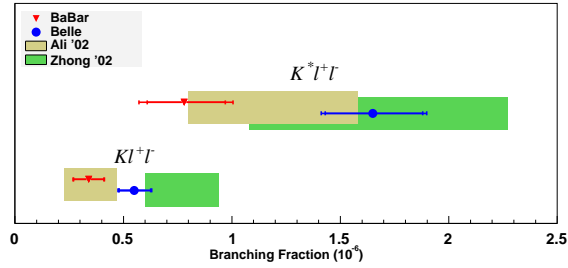


Figure 7: Summary of $B \rightarrow K \ell^+ \ell^-$ and $B \rightarrow K^* \ell^+ \ell^-$ branching fraction measurements.

four additional K^* modes (those with π^0 in the final state) and neural net event selection. The analysis of these modes has been divided into two discrete studies: (a) measurement of the K^* polarization (F_L) and the lepton forward-backward helicity angle asymmetry (A_{FB}) in $K^* \ell^+ \ell^-$ final states; and (b) measurement of the total inclusive $b \rightarrow s \ell^+ \ell^-$ rate using a sum-of-exclusive modes technique that leverages our group's prior experience in the semi-inclusive $b \rightarrow s \gamma$ analysis. F_L and A_{FB} provide theoretically clean observables in which to search for physics beyond the SM because their respective dependences on the mass of the di-lepton system in the final state have well-characterized SM predictions. Previous measurements of these observables by both Babar and Belle are highly statistics limited, with both collaborations reporting results that are generally in disagreement with the Standard Model at the 90% CL. The angular analysis is in the final stages of internal review by the collaboration, with the intention of presenting results at the upcoming FPCP 07 conference.

For Summer 2007, we anticipate presenting a preliminary analysis of the $b \rightarrow s \ell^+ \ell^-$ inclusive rate using the sum of exclusive modes technique, together with an update of the Spring 2007 angular analysis. These analyses will incorporate Run 6 data. The angular analysis will include a first-ever measurement of an additional angular observable $\Delta\phi$ (the angle between the K^* and di-lepton decay planes in $K^* \ell^+ \ell^-$ final states). In addition to the incremental increase in integrated luminosity, these analyses will benefit from the collaboration's reprocessing of the full Runs 1-5 BaBar dataset, which utilizes significantly upgraded charged track reconstruction algorithms. As with the angular analysis, theoretically clean SM predictions of the inclusive $b \rightarrow s \ell^+ \ell^-$ total and partial branching fractions are available, and measurements of these rates provide excellent opportunities to probe for the effects of New Physics.

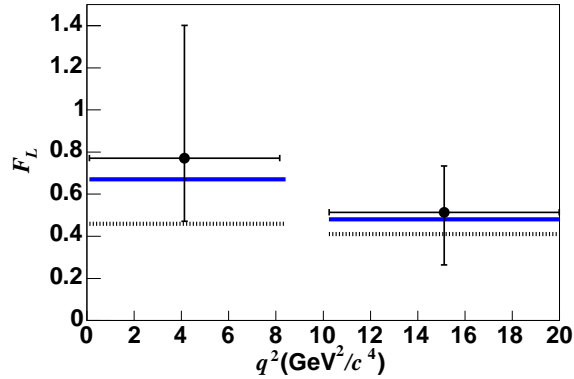


Figure 8: The measured fraction of longitudinal polarization of the K^* in $B \rightarrow K^* \ell^+ \ell^-$ decay is compared to the Standard Model (solid) and a beyond the SM predictions.

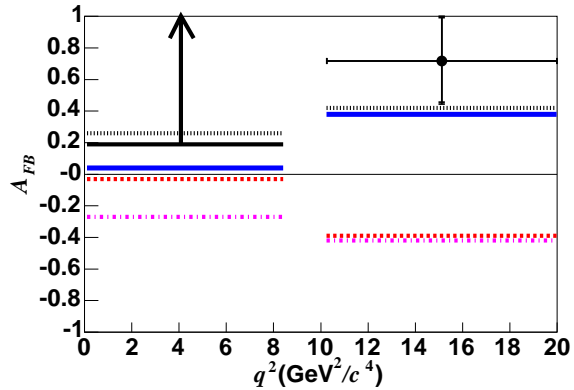


Figure 9: The measured forward backward asymmetry A_{FB} is compared to the Standard Model (solid) and some beyond the SM predictions.

2.3.5 Probing New Physics with $b \rightarrow s$ hadronic decays

M. Pierini has continued the study of time-dependent CP asymmetries in charmless B decays. Dominated by penguin diagrams, these channels are sensitive to virtual contributions from new heavy states (such as supersymmetric particles), which can shift the values of the CP parameters S and C far from the Standard Model expectations.

For the channel $B^0 \rightarrow K_S^0 \pi^0$ the fit to the data gives $S = 0.33 \pm 0.26 \pm 0.04$ and $C = 0.20 \pm 0.16 \pm 0.03$. The results are shown in Fig. 10 where the output of the time-dependent fit is superimposed on the data. These results were presented at Moriond 2007 and a publication with a update to the full data set (Runs 1-5) is planned.

The same vertexing technique was also applied to the update of $B^0 \rightarrow K_S^0 K_S^0 K_S^0$ with the Run 1-5 dataset (corresponding to 384 millions of $B\bar{B}$ pairs). Despite the fact that this channel is a three-body final state, the three kaons are forced into a pure CP-even state, because of the requirements of Bose statistics. This makes it possible to fit for the time-dependent CP asymmetry without reconstructing the intermediate resonances on the Dalitz plot. Since no tree-level contribution is present in the decay amplitude, in the absence of physics beyond the Standard Model one should measure $S = -\sin 2\beta \approx -0.68$ and $C \approx 0$. The analysis reconstructs signal events from the final states of three $K_S^0 \rightarrow \pi^+ \pi^-$ candidates or from events with two $K_S^0 \rightarrow \pi^+ \pi^-$ candidates and one $K_S^0 \rightarrow \pi^0 \pi^0$. The values of S , and C are obtained from a simultaneous fit to the two samples. The result, which was presented at Moriond 2007, gives $S = -0.71 \pm 0.24 \pm 0.04$ and

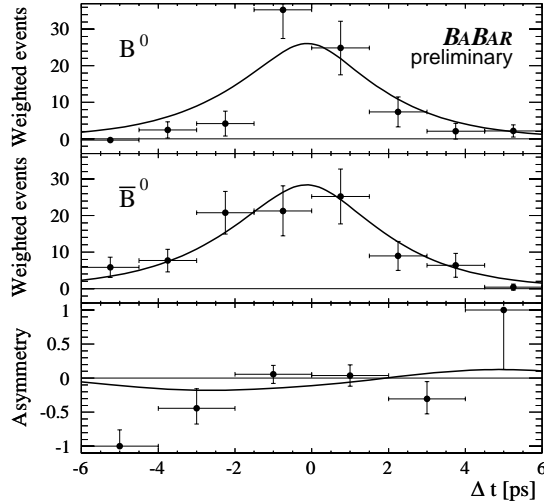


Figure 10: Time-dependent CP asymmetry for $B^0 \rightarrow K_S^0 \pi^0$ decays.

$C = 0.02 \pm 0.21 \pm 0.04$. Together with $B^0 \rightarrow \phi K_S^0$, this decay channel represents one of the most powerful probes of new physics in hadronic B decays. The present determination of time-dependent CP asymmetries in $b \rightarrow s$ decays is summarized in Fig. 11. Although these measurements do not provide a strong evidence of new physics, a combination of several such measurements can put interesting bounds on squark mixing processes in SUSY models.

The K_S^0 vertexing technique was also applied for the first time to $B^0 \rightarrow K_S^0 K_S^0$ decays. This transition is sensitive to $b \rightarrow d$ penguins, providing a complementary test of the Standard Model. On a sample of 348 million $B\bar{B}$ pairs, we observe the decays $B^0 \rightarrow K^0 \bar{K}^0$ with a statistical significance of 5σ , measuring $BR(B^0 \rightarrow K^0 \bar{K}^0) = (1.08 \pm 0.28 \pm 0.11) \times 10^{-6}$. With this sample, we determine $S = -1.28_{-0.73}^{+0.80} +0.11$ and $C = -0.40 \pm 0.41 \pm 0.06$.

Alternative searches of new physics at low energy were also performed with two analyses of leptonic decays. The first was a search for $B \rightarrow l^+ l^-$ decays ($l = e, \mu$) performed on the full Run 1-5 dataset. The event selection, based on BaBar $B \rightarrow hh$ analysis, uses PID requirements to separate hadronic and leptonic events. A fit to the hadronic events is done to extract the shape and the yield for continuum background, and this information is used to extract the yield of leptonic B decays. The analysis is will be completed by Summer 07. We expect to improve the previous Babar upper limit to obtain results which are comparable to the current best upper limit.

The second analysis consists of the search for violation of lepton universality in $\Upsilon(1S) \rightarrow ll$ decays $l = \mu, \tau$. This effect could be induced by new particles such as a light pseudoscalar Higgs. From LEP searches, there is a window for a light Higgs with mass between $7 \text{ GeV}/c^2$ and $10 \text{ GeV}/c^2$. If such a particle exists, it will be produced in the decay chain $\Upsilon(1S) \rightarrow H\gamma$, with $H \rightarrow ll$. Because the Yukawa couplings are flavour dependent, a breaking of lepton universality is introduced. This analysis uses a sample of $\Upsilon(1S)$ produced by initial state radiation (ISR) in e^+e^- collisions. Rather than reconstructing the radiative photon, which would strongly reduce the reconstruction efficiency, the analysis is done looking for $\Upsilon(2S)$ particles produced by ISR which decay to $\Upsilon(1S)\pi^+\pi^-$, with $\Upsilon(1S) \rightarrow ll$, while the $\pi^+\pi^-$ pair is used to tag the event. A previous analysis by CLEO reported a $\sim 2 \sigma$ deviation of lepton universality. With the data currently available at BaBar we plan to obtain an improved measurement of this quantity by summer 07.

2.3.6 Determination of $\bar{\rho}$ and $\bar{\eta}$ and bounds on New Physics

M. Pierini is a member of the UT_{fit} collaboration, which performs unitarity triangle fits and determines the CKM parameters $\bar{\rho}$ and $\bar{\eta}$. Using the new constraints from the measurements of Δm_s and $B \rightarrow \tau\nu$ and the CKM angles α , β , and γ , it is possible to test the Standard Model prediction for these quantities, as

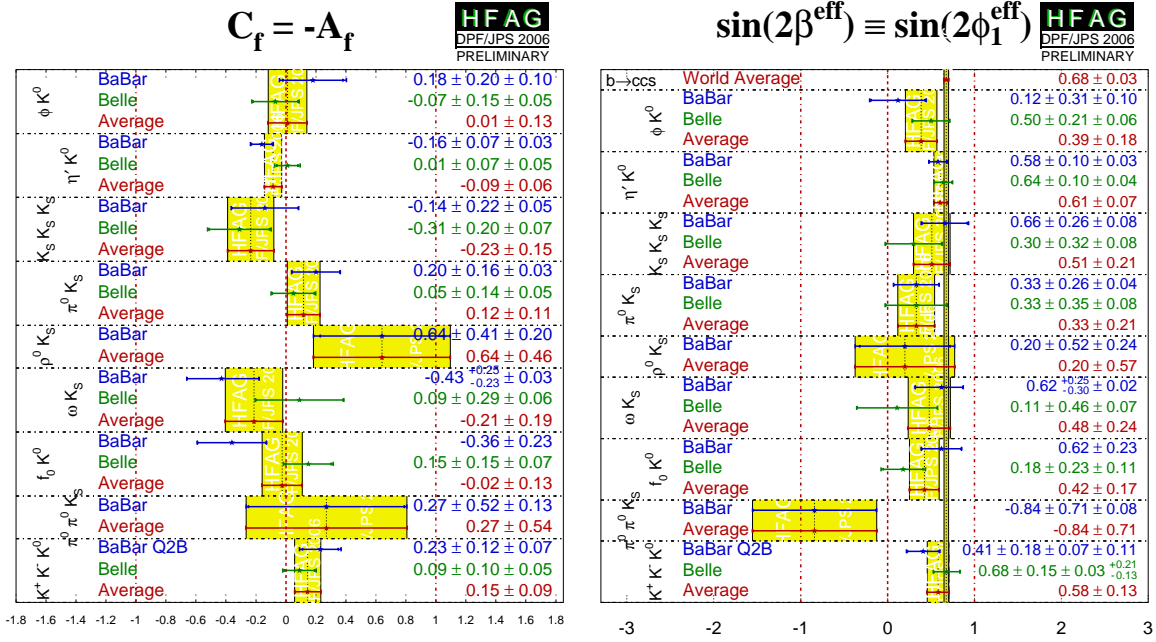


Figure 11: Status of measurements of S (left) and C (right) parameters for penguin-dominated $b \rightarrow s$ hadronic decays.

well as use them to validate predictions for factors and decay constants from lattice QCD. Combining all information, the Standard Model determination of the CKM parameters is obtained; $\bar{\rho} = 0.163 \pm 0.028$ and $\bar{\eta} = 0.344 \pm 0.016$. In addition, the abundance of available measurements permits a model independent fit of CKM parameters and new physics contributions to $B_{d,s} - \bar{B}_{d,s}$ and $K - \bar{K}$ mixing. The result, shown in the right hand plot of Fig. 12, proves that the Standard Model values of $\bar{\rho}$ and $\bar{\eta}$ describe the observed CP violation very well. Although there is a general consistency for the Standard Model expectation, there is a residual $\sim 2 \sigma$ deviation of the B_d mixing phase, due to an imperfect agreement between the measurements of V_{ub} and $\sin 2\beta$. If confirmed by future measurements, this inconsistency will provide evidence of new physics. Otherwise, the level of agreement with the SM fit will provide a lower value on the scale of new physics, with consequences for LHC direct searches for new heavy particles. The results are summarized in Pubs. 3, 14, 15, 16.

These analyses can translate the BaBar flavor physics program into constraints on New Physics parameters which are untestable at the LHC (such as squark mixing in SUSY models), underlining the complementarity of B-factories and LHC experiments.

2.3.7 Search for $D^0 \bar{D}^0$ -mixing

Postdoctoral associate K. Flood came to our group having set a limit on $D^0 \bar{D}^0$ -mixing using BaBar data collected through 2002. A new analysis of D -mixing using $D^{*+} \rightarrow \pi^+ D^0 (K^{(*)} e \nu)$ final states and $\sim 340 fb^{-1}$ of Runs 1-5 data ($\sim 4x$ the earlier dataset) has been completed and is in final review by the collaboration preparatory to submission to PRD. The larger dataset makes possible a new analysis technique which hadronically reconstructs the recoiling anti-charm partner of a mixed charm candidate decay in order to provide an independent flavor tag and additional kinematic constraints in reconstructing mixed signal candidates. The use of tagged events is relatively inefficient and results in a dataset comprised of only a few percent of all charm semileptonic decays, but yields a nearly background-free sample of mixed signal candidates. Figure 13 shows the $D^{*\pm} - D^0$ mass difference for mixed candidates obtained from the $\sim 340 fb^{-1}$ doubly flavor tagged sample. The dark histogram shows mixed events in the data passing all event selection cuts, while the light

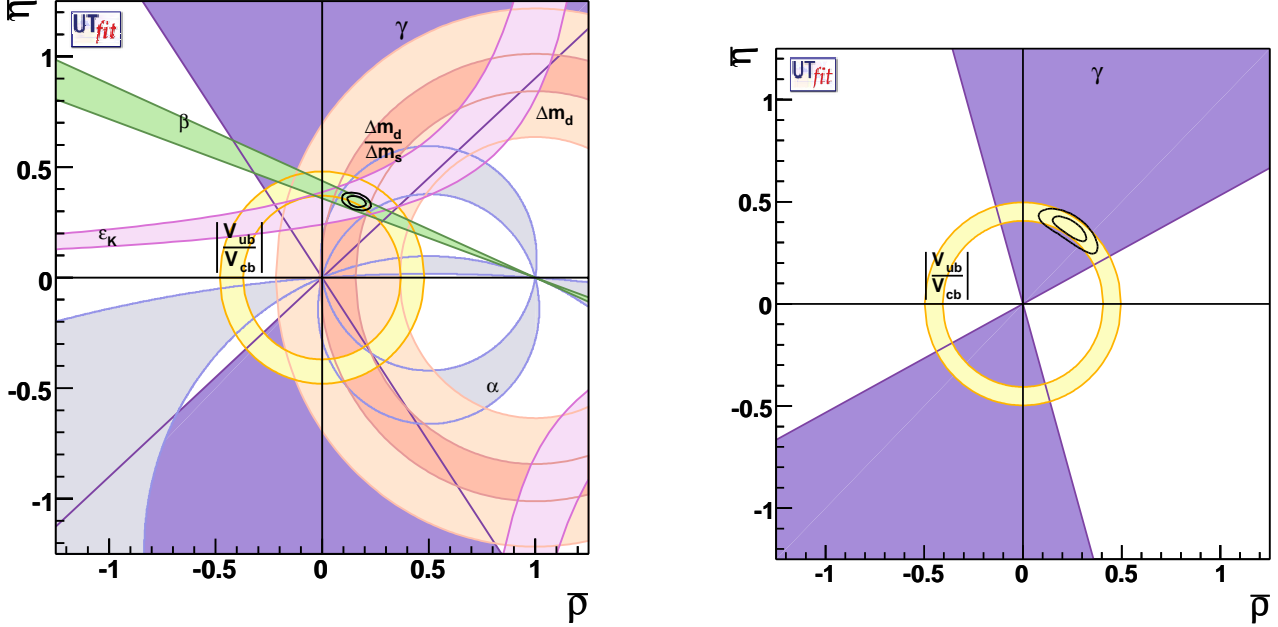


Figure 12: UT_{fit} determination of $\bar{\rho}$, $\bar{\eta}$ in the Standard Model (left) or allowing for New Physics contributions (right).

histogram shows mixed events passing a slightly looser event selection that allows a few sideband events to be obtained from the data in order to study the agreement of MC simulated and actual events. Region “1” on the plot is the signal region, and regions “2” and “3” are the near and far sidebands, respectively, used to estimate the background contribution to the signal region. Three mixed events are found in the data, with an expected contribution of 2.9 background events, yielding a mixing rate of 0.2×10^{-4} . A 90% CL upper limit of $< 0.12\%$ is obtained using a frequentist method that accounts for Poisson fluctuations in both data and simulated events, and conservatively assigns a 50% systematic to the estimation of the true background rate from simulated events. Using just 4x more data, the new limit is approximately 4x lower than the limit set by the 2002 analysis, demonstrating the utility of the recoil tagging technique. The central value for the semileptonic charm mixing result is in good agreement with the recent 4σ observation by BaBar of charm mixing using $D^0 \rightarrow K\pi$ final states (hep-ex/0703020, submitted to PRL). However, assuming that the $K\pi$ result is indicative of the actual mixing rate, there will only be an opportunity to observe mixing in semileptonic final states with the final BaBar dataset of about 900 fb^{-1} .

In addition to the overall mixing rate, the $K\pi$ charm mixing analysis finds a significant mixing contribution only in the lifetime difference of the weak eigenstates, with no contributions at all from the mass difference. Thus, mixing analyses which are uniquely sensitive to the lifetime difference are now the favored experimental systems with which to search for significant observations of charm mixing, and the use of the two-body CP-even $D^0 \rightarrow KK$ and $D^0 \rightarrow \pi\pi$ final states provide excellent opportunities to do just this. The recoil charm reconstruction technique pioneered in the semileptonic mixing analysis is a powerful technique that is generally applicable to a range of charm physics topics. When used to supplement a non-tagged CP-

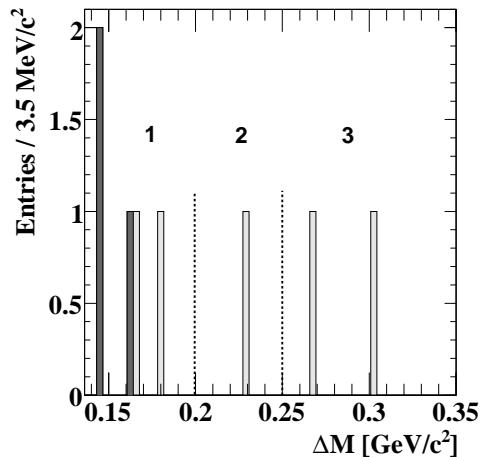


Figure 13: $D^{*\pm} - D$ mass difference for doubly flavor tagged mixed candidates.

even lifetime difference analysis, initial studies show that the use of tagged events will provide a potential doubling of the sensitivity to mixing in these modes, going from an expected $\sim 3 \sigma$ significant observation without tagging, to an expected $> 5 \sigma$ observation with tagging. We intend, therefore, to pursue the CP-even mixing analysis with the intention of presenting a result for the Lepton-Photon conference summer 07.

2.4 ILC Research and Development

2.4.1 Overview of the ILC Polarized Electron Source

In prior years a Wisconsin-SLAC collaboration developed polarized photocathodes which were used for the SLAC SLD and fixed target programs. Currently, the R&D program goal is the development of a polarized electron source (PES) which meets the ILC requirements for polarization, charge, lifetime, and pulse structure. There are two parts to this program. One part is the continued improvement of photocathode structures with higher polarization. The second part is the design and development of the laser system used to drive the photocathode. The long pulse train for the ILC introduces new challenges for the PES. More reliable and stable operation of the PES may be achievable if appropriate R&D is carried out for higher voltage operation and for a simpler photocathode load-lock system.

The collaboration with SLAC is through the Polarized Photocathode Research Collaboration (PPRC). Senior SLAC personnel include T. Maruyama, J. Clendenin, R. Kirby, and A. Brachmann.

The research to date has been successful in achieving higher polarization and higher QE, but the goal of $> 90\%$ polarization has not been achieved. The polarization appears saturated at 85% and a material-specific spin-depolarization mechanism appears to be present. Consequently, we have embarked on a program to study several types of superlattice structures.

2.4.2 Photocathode Development

After several years of intensive photocathode R&D, strained GaAs/GaAsP superlattice structures have emerged as the primary candidates for use with the ILC polarized electron source. Strained superlattice structures, consisting of very thin quantum well layers alternating with lattice-mismatched barrier layers are excellent candidates for achieving higher polarization since three issues are addressed. First, due to the difference in the effective mass of the heavy-holes and light-holes, the superlattice exhibits a natural splitting of the valence band, adding to the strain-induced contribution to the splitting. Secondly, each of the superlattice layers is thinner than the critical thickness. Thirdly, superlattice structures also have the additional advantage that they can overcome the inherent critical thickness limitation of single heterostructures, permitting a much thicker active layer for photoemission. The superlattice structures studied to date have all been designed with a high doping profile in a thin (10 nm) layer near the surface. The high surface

doping density is necessary to achieve high QE and to reduce the the surface-charge limit problem, while the lower doping density in the remaining 100 nm of the superlattice is required to reduce depolarization to a minimum. The surface-charge-limit problem was serious for the machines with warm accelerating structures which have a short bunch spacing of the order of nanoseconds. The relatively long bunch spacing of 300 ns for the cold ILC greatly reduces the surface-charge-limit problem and since there is an indication that the high surface doping density is limiting the peak polarization, the high-gradient-doping profile is being reevaluated.

Several types of new superlattice structures have been tested. A description of the progress follows.

InAlGaAs/GaAs Superlattice This structure is designed to have a flat conduction band, i.e. electrons do not have to tunnel through barriers as they diffuse to the surface. This structure was developed and tested by the Mamaev group at St. Petersburg University and showed a very high polarization of 92%. Samples from St. Petersburg were sent to SLAC to be measured by our group, but did not show the high polarization observed at St. Petersburg. The maximum polarization obtained for these samples with our measurements was consistent with 85% polarization. However, the measurements were made with a relatively high sample heat-cleaning temperature of 550° C. High temperature heat-cleaning generally results in performance degradation of the samples. The St. Petersburg samples were grown using Molecular Beam Epitaxy (MBE) which enabled them to arsenic cap the sample and use a lower heat cleaning temperature. To continue our study of this structure, two samples were ordered from SVT Associates in Minneapolis. After X-ray measurements and commercial Secondary Ion Mass Spectroscopy (SIMS) analysis the polarization and QE of these structures were measured in the SLAC test system. The results did not show the 92% polarization measured in St. Petersburg. The samples obtained from SVT were grown with chemical vapor deposition techniques (MOCVD) which precludes arsenic capping and consequently a high heat cleaning temperature of 550° again had to be used. We plan to obtain more samples and use a hydrogen cleaning technique which can be done at the lower temperature of 450°

InAlGaAs/GaAsP Superlattice This structure is designed to be strain compensated, i.e. the wells and barriers of the superlattice have almost equal and opposite strain, giving the benefits of the large heavy-hole light-hole splitting obtained from strain and a more ideally striated sample. Samples were obtained from the University of Sheffield in the UK. However the polarization measured by our group was only ~80%, not competitive with our best superlattice structures. No new samples are on order.

InGaP/GaAs Superlattice The goal in the design of this structure was to study the effect of lower spin-orbit coupling parameters. Samples were obtained through an SBIR award to SVT Associates. Three wafers were grown, two with a strained barrier, and one with a strained well. The highest polarization achieved was only 70% showing no improvement compared to our best photocathodes.

2.4.3 Photocathode Laser with the ILC Pulse Structure

In preparation for operating our developed photocathodes with the ILC pulse structure, Axel Brachmann of SLAC is developing a system to produce the required ILC 300 ns bunch spacing. The system uses a low power YAG/TiSaphire mode locked laser operating at 76 MHz which will be Pockels Cell switched to produce about a ms pulse with a 3 MHz microstructure. We have purchased a commercial Pockels Cell driver from Bergmann Messgerate Entwicklund KG capable of providing the 1 ms, 3 MHz structure as the first step in this program. SLAC has obtained the required Pockels cells. At a later date, an amplification stage will be added, giving sufficient power for photocathode photoemission.

2.4.4 ILC Detector Studies

H. Band was appointed as the muon working group co-leader together with E. Fisk of Fermilab for the SiD detector study concept. Several different technologies, scintillators or RPCs, can meet the present requirements. R&D plans to develop both the scintillator and RPC muon system designs are being made with the goal of selecting a preferred technology by the end of FY08. Resistive Plate Chambers (RPCs) of various types are the likely lowest cost option. RPCs, however, may have a nontrivial technical risk as demonstrated by problems experienced by the RPCs installed at the B Factory detectors. Choosing the

most reliable RPC technology for an ILC detector requires a thorough understanding of all aging issues and design problems.

Independent of the detector choice, some general design questions must be answered before an ILC muon system can be specified. The number of active layers, resolution, segmentation, and size directly affect both the cost of the detector and flux return steel, as well as the performance. Simulation efforts have begun within the Linear Collider Simulation framework to develop muon analysis packages and detector models.

1. RPC Aging

The 2nd generation BaBar RPCs have been much more reliable, particularly at the low rates expected for an ILC muon system. In four years of operation, low rate RPCs (rates $< 0.1\text{Hz}/\text{cm}^2$) still have an average efficiency over 95% as shown in Fig. 14a. BaBar observations of RPC aging suggested that pollutants produced in the gas in the highest rate areas were being transported to other regions and producing increased noise rates. One candidate for a gas-born pollutant is HF which can be produced by the disassociation of the Freon component in the RPC gas. Negative F ions in the RPC exhaust gas have been measured by ATLAS RPC aging studies and by BaBar. The lower charge per track of RPCs operated in avalanche mode compared with RPCs operated in streamer mode suggests that less F^- is produced in avalanche mode. To test this hypothesis measurements have been made in two RPCs, one operating in avalanche mode and the other operating in streamer mode. Since the F^- rate is dependent on the chamber noise rate, the amount of F^- production per day is plotted against the integrated RPC HV current in Fig. 14b for the RPC operating in avalanche mode and in Fig.14c for the RPC operating in streamer mode.

The F^- production rate for the streamer chamber was $1.42 \pm 0.11 \mu\text{mole}/\text{C}$. The F^- production rate for the avalanche chamber was $3.82 \pm 0.23 \mu\text{mole}/\text{C}$. The avalanche chamber produces more F^- per unit charge. However, since the average charge per track is lower by 4, the amount of Fluorine produced per track is $\sim 1/2$ that of a streamer mode chamber.

2. SiD Muon System Design Studies

Design studies have begun to estimate the cost of design decisions such as the number of detector layers or the thickness of the gap into which the detectors are inserted. Clearly the detector cost scales with area, however, the impact on the total weight of the detector is less obvious. If the total radial thickness of the steel is set to 3.2 m by the requirement to contain the return flux, the dependence of the total steel weight on the gap size or number of layers can be calculated as in Table 1. The total steel weight grows by 5.4% per cm of gap thickness. Reducing the number of layers from 23 to 14 reduces the detector weight by 500 metric tons, a cost savings of about 1.5 M\$ if the cost of steel is 3.5 \$/kg.

Other studies have estimated the average efficiency of one and two-layer RPC designs if the dead area due to edges and gas hoses is taken in account. For a single-layer design built from RPCs with a nominal efficiency of 90%, the average layer efficiency varied from 78-82% depending on the layer size. A double-gap RPC would have an average efficiency of 93%.

3 FUTURE PLANS

3.1 Overview

The major group activities will shift from BaBar support and analysis to detector and accelerator R&D for the ILC and CMS physics analysis over the course of this grant period. The Wisconsin group will continue to manage and support the RPC portion of the IFR until the end of data taking and the muon PID selectors until the end of BaBar physics analysis. R. Prepost will continue R&D for the ILC polarized electron source. H. Band and K. Flood will continue studies of ILC muon detector design and requirements with the aim of producing a SiD detector CDR in FY08 and an ILC detector EDR in FY10.

The electro-weak physics measurements, $b \rightarrow s\ell\ell$ (Food) and $B \rightarrow K\nu\nu$ (Vuosalu, Dasu) remain interesting through the end of BaBar data taking period because they are only limited by statistical precision. We expect to complete these measurements within a year of the end of BaBar data taking.

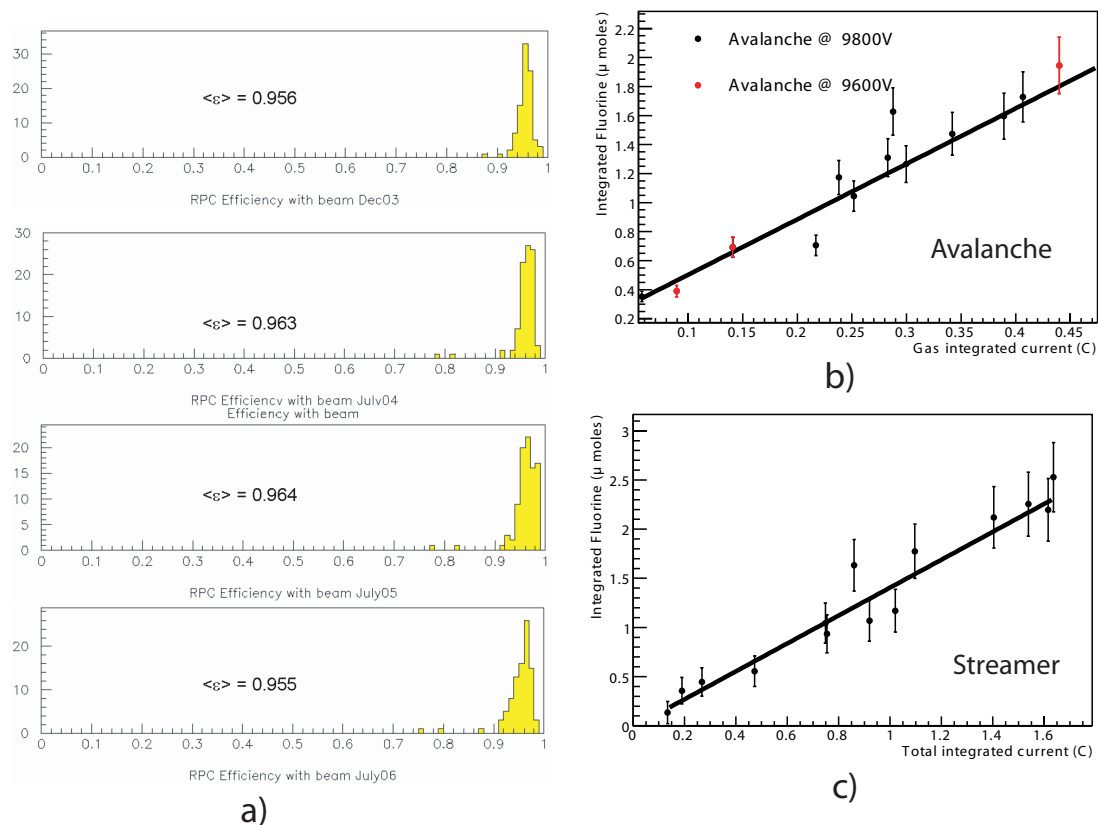


Figure 14: [a)] Efficiencies of BaBar RPCs in positions with the lowest backgrounds at Dec. 2003, July 2004, July 2005, and July 2006 measured by pairs in data. F^- production as a function of current for avalanche [b)] and streamer [c)] mode RPCs.

To further explore electro-weak physics Dasu, the new postdoc and students will set up a physics analysis group collocated with the CMS Tier-2 computing center at Madison and the Grid Laboratory of Wisconsin (GLOW), which are separately funded by the National Science Foundation. This group will define analysis strategies and establish the W and Z signatures with the first 1 fb^{-1} data in 2008, setting the stage for the Higgs boson searches, especially in the vector-boson fusion mode. The new postdoctoral associate will also be responsible for providing a gateway to this large opportunistic resource for ILC simulations.

4 BaBar

4.1 Support Activities

The final year of BaBar data taking will occur during FY08. Run 7 is scheduled from Dec. 07 to Sept. 08 which together with the present Run 6 is expected to more than double the BaBar data set from $\sim 400 \text{ fb}^{-1}$ to more than 900 fb^{-1} . The noise and signal rates will double as well (backgrounds are generally proportional to the luminosity) placing additional stress on the RPCs in the innermost and outer endcap layers. The access at the beginning of FY08 will be the last opportunity to modify the RPC chambers, electronics or background shielding to ensure that the endcap muon system remains efficient and reliable during this last crucial run. The avalanche mode conversion and changes in the background shielding will be completed during this final access if needed. The BaBar detector and the IFR will be kept intact during FY09.

Gap <i>cm</i>	0	3	4	5	23 ← <i>gaps</i>	3	4
R_{out} <i>m</i>	5.63	6.32	6.55	6.78	14 → <i>gaps</i>	6.05	6.19
Barrel <i>Metric tons</i>	3011	3253	3334	3414		3182	3239
Endcap <i>Metric tons</i>	3776	4758	5111	5476		4360	4564
Total <i>Metric tons</i>	6787	8011	8445	8890		7542	7833

Table 1: The expected weight and size of the SiD flux return steel as a function of the thickness of the gaps between the steel layers. The total radial steel thickness is set to 2.3 meters to return the flux of the 5 T solenoid. The yellow portion assumes 23 detector layers. The green portion assumes 14 layers.

The muon NN and BDT selectors will require training and validation for Run 6 and 7. If there is a complete reprocessing of the BaBar data set, the selectors will have to be retrained and revalidated for Runs 1-7. Studies of further improvements to IFR track reconstruction algorithms that may be implemented before final BaBar reprocessing have just begun.

4.2 Physics Analysis

The loop induced effects in the flavor sector provide tight constraints on the beyond the Standard Model physics. We find that constraints we are placing are relevant even in the LHC era. Further, the penguin mode measurements we made using BaBar data are often statistically limited, and can be improved with additional luminosity. The promise of increase in integrated luminosity from 200 fb^{-1} to 900 fb^{-1} by the end of BaBar data taking period, provides an opportunity to tighten these constraints enabling a thorough exploration of the phenomenological space of the new physics when it becomes directly accessible at LHC. Therefore, we propose to continue our efforts in measuring sensitive branching fraction and asymmetries in electroweak penguin processes.

The improved measurements will help constrain the flavor-mixing sector of New Physics and improve the experimental bounds on flavor-conserving new physics scenarios, for example the MSSM. In these Minimal Flavor Violation (MFV) models, no evidence of New Physics will appear in CP violation, but deviations from the expected decay rates of penguin and box-dominated rare decays (such as $B \rightarrow ll$, $B \rightarrow K\nu\bar{\nu}$, $b \rightarrow sll$, $b \rightarrow s\gamma$) will constrain model parameters.

Postdoctoral Associate K. Flood will continue the semi-inclusive analysis of $b \rightarrow s\ell^+\ell^-$ decays by combining the semi-inclusive technique that our group has pioneered in $b \rightarrow s\gamma$ analysis, and the improvements that he made to our muon identification software. He expects to integrate the signals from the new LST chambers that replace the aging RPC chambers in the Fall of 2006, to further improve the muon identification capability.

Our new student C. Vuosalo is measuring the currently poorly constrained $B \rightarrow K\nu\nu$ decay using the recoil technique, where one of the two B mesons in the $\Upsilon(4S)$ decay is fully reconstructed. This neutrino electro-weak penguin mode is experimentally more challenging than the charged lepton mode. Nevertheless, it is an interesting channel because it is theoretically clean involving only the weak coupling.

Our group participates in the overall BaBar physics program by participating in the analysis review process. The senior members of the group serve as members or the chairs of analysis review committees, which follow analyses from their initial stages all the way to the publication stage. The entire group also

participates in the final reviews of the publications.

4.3 ILC R&D

4.3.1 ILC Polarized Electron Source

Spin Relaxation Measurements using Faraday Rotation To date we have not had a technique to measure the spin relaxation time constants of the photocathode structures under test. To this end an apparatus to measure the photocathode polarization as a function of time using the Faraday Effect is under construction. The technique uses a pump-probe technique that first pumps electrons into the conduction band (pump pulse) with circularly polarized light to produce polarized electrons. The rotation of the linear polarization direction of a second linearly polarized light pulse (probe pulse) is measured as a function of the time delay between the pump and probe pulses. The rotation of the linear polarization angle due to the Faraday Effect is proportional to the degree of electron polarization and thus the electron polarization can be mapped as a function of time giving the spin relaxation time. The main apparatus component is a short pulse mode-locked Ti-S laser capable of producing pulse widths considerably shorter than the spin relaxation times to be measured. The laser wavelength spread also must be such that only the heavy-hole to conduction band transition is excited, required to produce the high polarization. To date we have acquired a Ti-S mode locked laser from KM labs and commissioning tests are under way. We plan to start making Faraday Rotation measurements in Spring-Summer 07. The direct measurement of spin relaxation times will help to identify the parameters most directly related to maximum photocathode polarization and lifetime.

InAlGaAs/GaAs Superlattice Studies The InAlGaAs/GaAs superlattice structure has a flat conduction band unlike other structures which have conduction band barriers for electron transport. As explained in the Technical Progress section, the lower measured polarization by our group relative to the polarization measurements made in St. Petersburg on the same structure is likely due to a higher heat cleaning temperature. We will obtain more wafers from the Mamaev group and implement low temperature atomic hydrogen cleaning.

InGaN Photocathode Studies The large band gap of InGaN offers the potential for structures with improved negative electron affinity (NEA) potentially yielding high quantum efficiency (QE) with a long lifetime. These are no other studies of the use of GaN based structures as a polarized photocathode. Preliminary samples were obtained through an SBIR award to SVT Associates. These studies will continue.

GaAs/GaAsP Superlattice We have continued to study the GaAs/GaAsP superlattice with the goal of optimizing the parameters with respect to doping concentration. Higher doping generally leads to depolarization effects and we would like to explore lower p-type doping levels. As stated earlier, the cold technology choice has greatly reduced the peak charge requirements and lower doping levels can be used. The GaAs/GaAsP superlattice structures which have been used for SLAC experiments have yielded 86% polarization and there should be a possibility for higher polarization. We plan to place an order for two samples with different doping levels from SVT Associates.

Laser with ILC Pulse Structure The Pockels cell driver required for production of the ILC pulse structure has arrived. The short term plan is to set up the laser system without the final stage amplifier in FY07/08 and later add the amplification stage to drive real photocathodes. There is currently an SBIR program with KM Labs to develop a suitable amplifier.

4.3.2 ILC Muon Detector and PID Studies

The US ILC Detector R&D plan continues to evolve. It will be highly desirable for the present 4 ILC detector concepts to coalesce into 2 complementary detector collaborations with detector EDRs by the time of the accelerator EDR in FY2010. The SiD concept collaboration hopes to complete a SiD Conceptual Design Report by FY08/09. As part of the SiD advisory board and co-coordinator for the muon system, H. Band will lead efforts to complete the SiD muon system design. In addition, Wisconsin will use its expertise with RPCs to study the aging characteristics of the several RPC types and to test suitable electronics.

Wisconsin will collaborate with the SLAC KPIX group to test prototypes of the SiD KPIX front end data acquisition chip in the readout of RPCs operating in the saturated avalanche mode. The SLAC group will provide several KPIX chips for testing and aid in the design of a chip carrier that will mate to the ~ 3 cm wide pickup strips of the RPCs. Initial tests of the device with existing BaBar RPC chambers will establish the compatibility and robustness of the present design with actual RPC signals. If successful, the tests will be extended to glass RPCs (as used in the HCAL prototype) and to chambers constructed from BESIII Bakelite RPCs.

Other studies will examine the production and absorption of F^- (HF) in glass and BESIII RPCs and compare them to standard RPCs with linseed oil. Previous studies have found clear correlations between contaminants such as HF and increased noise rates and currents. Bakelite RPCs have been found to be sensitive to both the input gas and environmental humidity. A study of the humidity sensitivity of RPCs constructed from BESIII Bakelite will help determine the optimal operating conditions for these chambers.

4.4 CMS Program in Task C

4.4.1 Overview

Recent progress in network enabled high-throughput computing has enabled university groups to conduct the majority of their research work while based on campus. S. Dasu established a productive collaboration with the UW computer sciences group, and is serving as the chair of the Technical Board for the Grid Laboratory of Wisconsin (GLOW) and as the manager of the CMS Tier-2 computing center in Madison. In addition to ~ 1000 state-of-the-art CPUs, the Tier-2 center is also building up to host reconstructed CMS data in a 200-TB storage system. The UW Tier-2 center is already one of the best places to perform CMS physics studies. The Tier-2 and GLOW facilities are supported by CMS project and NSF-MRI funds. The Condor group in the CS department provides valuable advice and help as needed. It is important that we leverage this resource. Therefore, we propose to build a strong physics analysis group at Madison collocated with the Tier-2 center. This is mutually beneficial to Tier-2 operations and our physics analysis teams at Madison and those based at Geneva to work on the trigger and muon systems hardware.

Specifically, we would like to hire one postdoctoral researcher to replace M. Pierini. The duties of the postdoc will include debugging and upkeep of the Tier-2 analysis environment by maintaining a working physics analysis at all times. The postdoctoral researcher will also mentor graduate students in developing analyses and provide technical assistance to the Tier-2 users. Graduate student Mike Anderson, who is currently supported on university funds, has experience setting up analysis at our Tier-2 and has established an analysis. Incoming students Gray and Bachtis have also expressed interest in CMS work, but they will be supported on University funds initially. This team working under the supervision of S. Dasu, will also work in the area of computing, neural networks and statistical pattern recognition based particle ID technology. The muon ID techniques developed by our group for BaBar provide a good starting point for the CMS work.

At the 25% level, the postdoc will also maintain the ILC/SiD software base and participate in simulations of the muon system design under the supervision of H. Band. The SiD design effort will be able to opportunistically use the GLOW resources and any unused resources in the CMS Tier-2. We will ensure that the postdoc time is divided among the two tasks such that there is an effective contribution to both the projects.

4.4.2 Physics Analysis

S. Dasu has developed calorimetric hardware triggers and online selection strategies for vector boson and Higgs decays to τ -pairs. He is now focussing on data analysis issues, especially on analyzing the initial 1 fb^{-1} data to be collected in 2008. He will continue his work in configuring the trigger and online selection for studying vector boson τ -decays to tune the τ identification and calibration. Of particular interest is $Z \rightarrow \tau\tau$ production via the electro-weak process, in which vector bosons radiated from the quark lines fuse to produce the Z or Higgs. The forward going quarks hadronize into jets that can be measured within the acceptance of the CMS calorimeter. The lack of color connection between the two final state quarks results in a quiet calorimeter in the central region. This is a promising mode for Higgs boson studies. Establishing our ability to see Z decays to τ -pairs and via a vector boson fusion signature (forward tag jets accompanied by highly suppressed central hadronic activity) during low luminosity is a precursor to the search for Higgs

in the vector boson fusion process, where the produced Higgs decays to a pair of taus through its Yukawa coupling. Preliminary studies have shown that the 30 fb^{-1} data that we hope to collect by 2010 will yield this signal. Even if a Higgs boson is discovered in some other channel, this signal remains an important process for measuring the Yukawa couplings. There is also interest in τ -channels in the searches for the MSSM heavy and charged Higgs bosons.

Last year M. Anderson began learning CMS software and participated in the establishing analysis at our Tier-2. He developed an analysis of $H \rightarrow \gamma\gamma$ decays to reproduce past CMS studies in the new software framework. He will complete this feasibility study this summer to obtain dissertator status. He will then concentrate on photon reconstruction and study π^0 contamination. Powerful multi-variate techniques that our group pioneered can be very useful in photon identification with CMS. Study of high E_T photon and diphoton spectra is of interest even with initial 1 fb^{-1} data.

5 BUDGET DESCRIPTION

The faculty level of Prepost and Dasu remains unchanged. The scientific staff level remains unchanged with Senior Scientist Band and Post-doctoral Associates K. Flood and a replacement for M. Pierini who leaves the group at the end of April 07 to take up a CERN fellowship. We expect to divide the 2 FTE post doctoral effort such that approximately 0.75 FTE is in BaBar, 0.5 FTE is in ILC and 0.75 FTE is in CMS, tailored to maximize the postdoc career prospects while satisfying our ILC research needs. Currently there is one BaBar graduate student, C. Vuosalo, who started in 6/06. The budget also includes support twelve months of CMS graduate student, M. Anderson, who also started in 6/06 but was supported by university funds. Incoming students M. Bachtis and L. Gray will be supported by university funds initially.

The FY2008 budget request includes a \$15k foreign travel item for collaboration meetings and conferences outside the US based on four collaboration meetings and four conferences for Prepost, Dasu, Band and Flood. For domestic travel and domestic conference expenses we request \$10k for the SLAC services contract.

The ILC polarized source development program continues to focus on the further development of high current cathodes meeting ILC specifications and the development of the laser system for the ILC polarized electron source. A proposal entitled "Development of Polarized Photocathodes for the Linear Collider" was submitted to the University Consortium for a Linear Collider in Oct. 2003, requesting \$34.6k per year of R&D funds. The proposal was approved for three year funding in Oct. 2004.

A separate proposal, "RPC and Muon System Studies" has been made to the ILC University-based Linear Collider Detector R&D program (FY2007) by H. Band and K. Flood to procure funding for test equipment, etc.. This additional grant is necessary to meet the ambitious goal of producing a detector EDR on the same time scale (FY2010) as the GDE accelerator EDR. In particular, this grant would supply additional resources are needed in FY08 for the proposed SiD detector CDR.

6 PERSONNEL

PERSONNEL DISTRIBUTION							
Grant Period: Nov.1, 2007 - Oct. 31 2010							
University of Wisconsin							
TASK C							
Position	Name	Activity			Months	Advisor	Comments
		Babar	ILC	CMS			
Faculty	R. Prepost	20	80		2		
	S. Dasu	20		80	2		one month in Task T
Res. Sci.	H. Band	40	60		12		
Postdoc	K. Flood	75	25		12		
	Pierini Replacement		25	75	12		
Grad. Stud.	C. Vuosalo	100			12	Dasu	
	M. Anderson			100	12	Dasu	(starts 06//2007)

7 PUBLICATIONS AND CONFERENCE PRESENTATIONS

Books

1. “Muonium–The Early Experiments”, R. Prepost in *Proceedings of the Memorial Symposium in Honor of Vernon Willard Hughes*, edited by E. Hughes and F. Iachello (World Scientific, Singapore, 2004).

Publications 2008 - 2006

2008

1. B. Aubert *et al.* [BABAR Collaboration], “Time-dependent Dalitz plot analysis of $B^0 \rightarrow D^{(-)} K^0 \pi^{+(-)}$ decays,” *Phys. Rev. D* **77**, 071102 (2008).
2. B. Aubert *et al.* [BABAR Collaboration], “Measurement of the $B \rightarrow X_s \gamma$ Branching Fraction and Photon Energy Spectrum using the Recoil Method,” *Phys. Rev. D* **77**, 051103 (2008).
3. B. Aubert *et al.* [BABAR Collaboration], “Search for CPT and Lorentz Violation in B^0 - B^0 bar Oscillations with Dilepton Events,” *Phys. Rev. Lett.* **100**, 131802 (2008).
4. B. Aubert *et al.* [BABAR Collaboration], “Search for Lepton Flavor Violating Decays $\tau^\pm \rightarrow l^\pm \omega$ ($l = e, \mu$),” *Phys. Rev. Lett.* **100**, 071802 (2008).
5. B. Aubert *et al.* [BaBar Collaboration], “A study of $\bar{B} \rightarrow \Xi_c^- A_c^-$ and $\bar{B} \rightarrow \Lambda_c^+ A_c^- \bar{K}$ decays at BABAR,” *Phys. Rev. D* **77**, 031101 (2008).
6. B. Aubert *et al.* [BABAR Collaboration], “Observation of B^+ Meson Decays $\rightarrow a_1(1260)^+ K^0$ and $B^0 \rightarrow a_1(1260) - K^+$,” *Phys. Rev. Lett.* **100**, 051803 (2008).
7. B. Aubert *et al.* [BABAR Collaboration], “Observation of $B^0 \rightarrow K^{*0} K^{*0}$ bar and search for $B^0 \rightarrow K^{*0} K^{*0}$,” *Phys. Rev. Lett.* **100**, 081801 (2008).
8. B. Aubert *et al.* [BABAR Collaboration], “Measurement of the CP-Violating Asymmetries in $B^0 \rightarrow K_S \pi^0$ and of the Branching Fraction of $B^0 \rightarrow K^0 \pi^0$,” *Phys. Rev. D* **77**, 012003 (2008).
9. B. Aubert *et al.* [BABAR Collaboration], “Determination of the Form Factors for the Decay $B^0 \rightarrow D^{*-} l + \nu_l$ and of the CKM Matrix Element $|V_{cb}|$,” *Phys. Rev. D* **77**, 032002 (2008).

10. B. Aubert *et al.* [BABAR Collaboration], “Measurement of the absolute branching fraction of $D0 \rightarrow K^- \pi^+$,” *Phys. Rev. Lett.* **100**, 051802 (2008).
11. B. Aubert *et al.* [BaBar Collaboration], “Study of $B0 \rightarrow l+l'$ - decays ($l,l' = e,\mu$),” *Phys. Rev. D* **77**, 032007 (2008).
12. B. Aubert *et al.* [BaBar Collaboration], “A study of $Bbar \rightarrow \Xi_c A_c^-$ and $Bbar \rightarrow \Lambda_c^+ \Lambda_c^-$ Kbar decays at BABAR,” *Phys. Rev. D* **77**, 031101 (2008).
13. B. Aubert *et al.* [BABAR Collaboration], “A Study of Excited Charm-Strange Baryons with Evidence for new Baryons $\Xi_c(3055)^+$ and $\Xi_c(3123)^+$,” *Phys. Rev. D* **77**, 012002 (2008).
14. B. Aubert *et al.* [BaBar Collaboration], “Search for CP Violation in the Decays $D0 \rightarrow K^- K^+$ and $D0 \rightarrow \pi^- \pi^+$,” *Phys. Rev. Lett.* **100**, 061803 (2008).
15. B. Aubert *et al.* [BABAR Collaboration], “Observation of the Semileptonic Decays $B \rightarrow D^*$ tau nubar and Evidence for $B \rightarrow D$ tau nubar,” *Phys. Rev. Lett.* **100**, 021801 (2008).
16. B. Aubert *et al.* [BABAR Collaboration], “A search for $B^+ \rightarrow \tau^+ \nu$ with Hadronic B tags,” *Phys. Rev. D* **77**, 011107 (2008).
17. B. Aubert *et al.* [BABAR Collaboration], “Study of Resonances in Exclusive B Decays to $Dbar(*)D(*)K$,” *Phys. Rev. D* **77**, 011102 (2008).
18. B. Aubert *et al.* [The BABAR Collaboration], “Search for the rare charmless hadronic decay $B^+ \rightarrow a0^+ \pi0$,” *Phys. Rev. D* **77**, 011101 (2008) [Erratum-ibid. *D* **77**, 039903 (2008) ERRAT,D77,019904.2008].
19. B. Aubert *et al.* [BABAR Collaboration], “Exclusive branching fraction measurements of semileptonic tau decays into three charged hadrons, $\tau^- \rightarrow \phi \pi^- \nu_\tau$ and $\tau^- \rightarrow \phi K^- \nu_\tau$,” *Phys. Rev. Lett.* **100**, 011801 (2008).
20. B. Aubert *et al.* [BABAR Collaboration], “Search for the Decays $B0 \rightarrow e+e-\gamma$ and $B0 \rightarrow \mu+\mu-\gamma$,” *Phys. Rev. D* **77**, 011104 (2008).

2007

21. M. Ciuchini, M. Pierini, and L. Silvestrini, “Hunting the CKM Weak Phase with Time-Integrated Dalitz Plot Analyses of $B(s) \rightarrow K K \pi$ and $B(s) \rightarrow K \pi \pi$ Decays”, *Phys. Lett.* **B645**, 201 (2007).
22. B. Aubert *et al.* [BABAR Collaboration], “Study of $e+e- \rightarrow A\bar{A}, A\bar{\Sigma}^0, \Sigma^0\bar{\Sigma}^0$ using Initial State Radiation with BABAR,” *Phys. Rev. D* **76**, 092006 (2007).
23. B. Aubert *et al.* [BABAR Collaboration], “Improved Limits on the Lepton-Flavor Violating Decays $\tau^- \rightarrow l-l-$,” *Phys. Rev. Lett.* **99**, 251803 (2007).
24. B. Aubert *et al.* [BABAR Collaboration], “Measurements of the Branching Fractions of $B0 \rightarrow K^*0K^+K^-$, $B0 \rightarrow K^*0\pi^+K^-$, $B0 \rightarrow K^*0K^+\pi^-$, and $B0 \rightarrow K^*0\pi^+\pi^-$,” *Phys. Rev. D* **76**, 071104 (2007).
25. B. Aubert *et al.* [BABAR Collaboration], “The $e^+e^- \rightarrow 2(\pi^+\pi^-)\pi^0, 2(\pi^+\pi^-)\eta, K^+K^-\pi^+\pi^-\pi^0$ and $K^+K^-\pi^+\pi^-\eta$ Cross Sections Measured with Initial-State Radiation,” *Phys. Rev. D* **76**, 092005 (2007).
26. B. Aubert *et al.* [BaBar Collaboration], “Improved Measurement of Time-Dependent CP Asymmetries and the CP-Odd Fraction in the Decay $B^0 \rightarrow D^{*+}D^{*-}$,” *Phys. Rev. D* **76**, 111102 (2007).
27. B. Aubert *et al.* [BABAR Collaboration], “Measurement of $\cos 2\beta$ in $B0 \rightarrow D(*)h0$ Decays with a Time-Dependent Dalitz Plot Analysis of $D \rightarrow K S \pi^+ \pi^-$,” *Phys. Rev. Lett.* **99**, 231802 (2007).
28. B. Aubert *et al.* [BABAR Collaboration], “Search for the decay $B^+ \rightarrow K^+ \tau^- / + \mu^- / -$,” *Phys. Rev. Lett.* **99**, 201801 (2007).

29. B. Aubert *et al.* [BABAR Collaboration], “Observation of the Decay $B^+ \rightarrow K+K\text{-}\pi^+$,” *Phys. Rev. Lett.* **99**, 221801 (2007).
30. B. Aubert *et al.* [The BABAR Collaboration], “Search for $b \rightarrow u$ transitions in $B^- \rightarrow [K^+\pi^-\pi^0]_D K^-$,” *Phys. Rev. D* **76**, 111101 (2007).
31. B. Aubert *et al.* [BABAR Collaboration], “Evidence for charged B meson decays to $a_1(1260)\text{+/-}\pi^0$ and $a_1(1260)0\pi^{\text{+/-}}$,” *Phys. Rev. Lett.* **99**, 261801 (2007).
32. B. Aubert *et al.* [The BABAR Collaboration], “Observation of B-meson decays to $b(1)\pi$ and $b(1)K$,” *Phys. Rev. Lett.* **99**, 241803 (2007).
33. B. Aubert *et al.* [BABAR Collaboration], “Measurement of the $\tau^- \rightarrow K^-\pi^0\nu_\tau$ Branching Fraction,” *Phys. Rev. D* **76**, 051104 (2007).
34. B. Aubert *et al.* [BABAR Collaboration], “Study of $B^0 \rightarrow \pi^0\pi^0$, $B \rightarrow \pi\pi^0$, and $B \rightarrow K\pi^0$ Decays, and Isospin Analysis of $B \rightarrow \pi\pi$ Decays,” *Phys. Rev. D* **76**, 091102 (2007).
35. B. Aubert *et al.* [BaBar Collaboration], “Evidence for the $B^0 \rightarrow p\bar{p}K^{*0}$ and $B^+ \rightarrow \eta_c K^{*+}$ decays and Study of the Decay Dynamics of B Meson Decays into $p\bar{p}$ Final States,” *Phys. Rev. D* **76**, 092004 (2007)
36. B. Aubert *et al.* [BABAR Collaboration], “Search for Prompt Production of χ_c and X(3872) in e^+e^- Annihilations,” *Phys. Rev. D* **76**, 071102 (2007).
37. B. Aubert *et al.* [BABAR Collaboration], “Branching fraction and CP-violation charge asymmetry measurements for B-meson decays to $\eta K^{\text{+/-}}$, $\eta\pi^{\text{+/-}}$, $\eta'K$, $\eta'\pi^{\text{+/-}}$, ωK , and $\omega\pi^{\text{+/-}}$,” *Phys. Rev. D* **76**, 031103 (2007).
38. B. Aubert *et al.* [BABAR Collaboration], “Measurements of CP-Violating Asymmetries in the Decay $B^0 \rightarrow K+K\text{-}K^0$,” *Phys. Rev. Lett.* **99**, 161802 (2007).
39. B. Aubert *et al.* [BABAR Collaboration], “Evidence of a broad structure at an invariant mass of $4.32\text{-GeV}/c^{**2}$ in the reaction $e^+e^- \rightarrow \pi^+\pi^-\psi(2S)$ measured at BaBar,” *Phys. Rev. Lett.* **98**, 212001 (2007).
40. B. Aubert *et al.* [BABAR Collaboration], “Search for lepton flavor violating decays $\tau^{\text{+/-}} \rightarrow l^{\text{+/-}}\pi^0$, $l^{\text{+/-}}\eta$, $l^{\text{+/-}}\eta'$,” *Phys. Rev. Lett.* **98**, 061803 (2007).
41. B. Aubert *et al.* [BABAR Collaboration], “Evidence for the rare decay $B^+ \rightarrow D/s^+\pi^0$,” *Phys. Rev. Lett.* **98**, 171801 (2007).
42. B. Aubert *et al.* [BABAR Collaboration], “Measurement of B decays to $\Phi K\gamma$,” *Phys. Rev. D* **75**, 051102 (2007).
43. B. Aubert *et al.* [BABAR Collaboration], “Branching fraction measurements of $B^+ \rightarrow \rho^+\gamma$, $B^0 \rightarrow \rho^0\gamma$, and $B^0 \rightarrow \omega\gamma$,” *Phys. Rev. Lett.* **98**, 151802 (2007).
44. B. Aubert *et al.* [BABAR Collaboration], “Measurement of the $B^0 \rightarrow \pi^+l^+\nu$ form-factor shape and branching fraction, and determination of $-V(\text{ub})-$ with a loose neutrino reconstruction technique,” *Phys. Rev. Lett.* **98**, 091801 (2007).
45. B. Aubert *et al.* [BABAR Collaboration], “Evidence for $B^0 \rightarrow \rho^0\rho^0$ decay and implications for the CKM angle α ,” *Phys. Rev. Lett.* **98**, 111801 (2007).
46. B. Aubert *et al.* [BABAR Collaboration], “Measurements of CP-violating asymmetries in $B^0 \rightarrow a_1(1260)\text{+/-}\pi^{\text{+/-}}$ decays,” *Phys. Rev. Lett.* **98**, 181803 (2007).
47. B. Aubert *et al.* [BABAR Collaboration], “Measurement of the $B^{\text{+/-}} \rightarrow \rho^{\text{+/-}}\pi^0$ branching fraction and direct CP asymmetry,” *Phys. Rev. D* **75**, 091103 (2007).

48. B. Aubert *et al.* [BABAR Collaboration], “Measurement of CP asymmetry in $B^0 \rightarrow K^0(S) \pi^0 \pi^0$ decays,” *Phys. Rev. D* **76**, 071101 (2007).
49. B. Aubert *et al.* [BaBar Collaboration], “Observation of $B^+ \rightarrow \rho^+ K^0$ and measurement of its branching fraction and charge asymmetry,” *Phys. Rev. D* **76**, 011103 (2007).
50. B. Aubert *et al.* [BABAR Collaboration], “Measurement of CP Asymmetries in $B^0 \rightarrow K^0_S K^0_S K^0_S$ Decays,” *Phys. Rev. D* **76**, 091101 (2007).
51. B. Aubert *et al.* [BABAR Collaboration], “Measurement of CP-violating asymmetries in $B^0 \rightarrow (\rho \pi)^0$ using a time-dependent Dalitz plot analysis,” *Phys. Rev. D* **76**, 012004 (2007).
52. B. Aubert *et al.* [BABAR Collaboration], “Observation of CP violation in $B^0 \rightarrow K^+ \pi^-$ and $B^0 \rightarrow \pi^+ \pi^-$,” *Phys. Rev. Lett.* **99**, 021603 (2007).
53. B. Aubert *et al.* [BABAR Collaboration], “Search for the rare decay B to $\pi^+ l^+ l^-$,” *Phys. Rev. Lett.* **99**, 051801 (2007).
54. B. Aubert *et al.* [BABAR Collaboration], “Measurement of the time-dependent CP asymmetry in $B^0 \rightarrow D^{(*)0}(\text{CP}) h^0$ decays,” *Phys. Rev. Lett.* **99**, 081801 (2007).
55. B. Aubert *et al.* [BABAR Collaboration], “Evidence for D^0 - anti- D^0 mixing,” *Phys. Rev. Lett.* **98**, 211802 (2007).
56. B. Aubert *et al.* [BABAR Collaboration], “Improved Measurement of CP Violation in Neutral B Decays to $c \bar{c} s$,” *Phys. Rev. Lett.* **99**, 171803 (2007).
57. B. Aubert *et al.* [BABAR Collaboration], “Measurement of the relative branching fractions of anti- $B \rightarrow D / D^* / D^{**} l^- \text{ anti-}\nu/l$ decays in events with a fully reconstructed B meson,” *Phys. Rev. D* **76**, 051101 (2007).
58. B. Aubert *et al.* [BABAR Collaboration], “Production and decay of Ω_c^0 ,” *Phys. Rev. Lett.* **99**, 062001 (2007).
59. B. Aubert *et al.* [BaBar Collaboration], “Measurement of CP violation parameters with a Dalitz plot analysis of $B^{+-} \rightarrow D(\pi^+ \pi^- \pi^0) K^{+-}$,” *Phys. Rev. Lett.* **99**, 251801 (2007).
60. B. Aubert *et al.* [BABAR Collaboration], “Search for neutral B-meson decays to $a^0 \pi$, $a^0 K$, $\eta \rho^0$, and ηf_0 ,” *Phys. Rev. D* **75**, 111102 (2007).
61. B. Aubert *et al.* [BABAR Collaboration], “The $e^+e^- \rightarrow K^+K^-\pi^+\pi^-$, $K^+K^-\pi^0\pi^0$ and $K^+K^-K^+K^-$ Cross Sections Measured with Initial-State Radiation,” *Phys. Rev. D* **76**, 012008 (2007).
62. B. Aubert *et al.* [BABAR Collaboration], “Measurement of decay amplitudes of $B \rightarrow J / \psi K^*$, $\psi(2S) K^*$, and $\chi(c1) K^*$ with an angular analysis,” *Phys. Rev. D* **76**, 031102 (2007).
63. B. Aubert *et al.* [BABAR Collaboration], “Branching fraction and charge asymmetry measurements in $B \rightarrow J/\psi \pi^+ \pi^-$ decays,” *Phys. Rev. D* **76**, 031101 (2007).
64. B. Aubert *et al.* [BABAR Collaboration], “Measurement of the absolute branching fraction of $D^0 \rightarrow K^- \pi^+$,” *Phys. Rev. Lett.* **100**, 051802 (2008).
65. B. Aubert *et al.* [BABAR Collaboration], “Amplitude Analysis of the decay $D^0 \rightarrow K^- K^+ \pi^0$,” *Phys. Rev. D* **76**, 011102 (2007).
66. B. Aubert *et al.* [BABAR Collaboration], “Search for $B^0 \rightarrow \Phi(K^+ \pi^-)$ decays with large K^+ π^- invariant mass,” *Phys. Rev. D* **76**, 051103 (2007).
67. B. Aubert *et al.* [BABAR Collaboration], “Search for D^0 - anti- D^0 mixing using doubly flavor tagged semileptonic decay modes,” *Phys. Rev. D* **76**, 014018 (2007).

68. B. Aubert *et al.* [BaBar Collaboration], “Measurement of CP-Violating Asymmetries in $B^0 \rightarrow D^{(*)\pm} D^\mp$,” Phys. Rev. Lett. **99**, 071801 (2007).
69. B. Aubert *et al.* [BABAR Collaboration], “A search for $B^+ \rightarrow \tau^+ \nu$,” Phys. Rev. D **76**, 052002 (2007).
70. B. Aubert *et al.* [Babar Collaboration], “A Study of B^0 to $\rho^+\rho^-$ Decays and Constraints on the CKM Angle α ,” Phys. Rev. D **76**, 052007 (2007).
71. B. Aubert *et al.* [The BaBar Collaboration], “Search for the decay $B^+ \rightarrow \bar{K}^0(892) K^+$,” Phys. Rev. D **76**, 071103 (2007).
72. B. Aubert *et al.* [BABAR Collaboration], “Measurement of the Decay $B^- \rightarrow D^*0 e^- \bar{\nu}$,”
73. B. Aubert *et al.* [BABAR Collaboration], “Vector - tensor and vector - vector decay amplitude analysis of $B^0 \rightarrow \Phi K^*0$,” Phys. Rev. Lett. **98**, 051801 (2007).
74. B. Aubert *et al.* [BABAR Collaboration], “Branching fraction measurement of anti- $B^0 \rightarrow D^{(*)+} \pi^-$, $B^- \rightarrow D^{(*)0} \pi^-$ and isospin analysis of anti- $B \rightarrow D^{(*)} \pi$ decays,” Phys. Rev. D **75**, 031101 (2007).
75. B. Aubert *et al.* [BABAR Collaboration], “Observation of CP violation in $B^0 \rightarrow \eta' K^0$ decays,” Phys. Rev. Lett. **98**, 031801 (2007).
76. B. Aubert *et al.* [BABAR Collaboration], “Inclusive Λ/c production in $e^+ e^-$ annihilations at $s^{*1/2} = 10.54$ -GeV and in $\Upsilon(4S)$ decays,” Phys. Rev. D **75**, 012003 (2007).
77. B. Aubert *et al.* [BABAR Collaboration], “Measurement of the CP asymmetry and branching fraction of $B^0 \rightarrow \rho^0 K^0$,” Phys. Rev. Lett. **98**, 051803 (2007).
78. B. Aubert *et al.* [BABAR Collaboration], “Observation of $B \rightarrow \eta' K^*$ and evidence for $B^+ \rightarrow \eta' \rho^+$,” Phys. Rev. Lett. **98**, 051802 (2007).
79. B. Aubert *et al.* [BABAR Collaboration], “Search for the reactions $e^+ e^- \rightarrow \mu^+ \tau^-$ and $e^+ e^- \rightarrow e^+ \tau^-$,” Phys. Rev. D **75**, 031103 (2007).
80. B. Aubert *et al.* [BABAR Collaboration], “Improved measurements of the branching fractions for $B^0 \rightarrow \pi^+ \pi^-$ and $B^0 \rightarrow K^+ \pi^-$, and a search for $B^0 \rightarrow K^+ K^-$,” Phys. Rev. D **75**, 012008 (2007).

2006

81. H. R. Band *et al.*, “Performance And Aging Studies Of Babar Resistive Plate Chambers,” Nucl. Phys. Proc. Suppl. **158**, 139 (2006).
82. W. M. Yao *et al.* [Particle Data Group], “Review of Particle Physics,” J. Phys. G **33**, 1 (2006).
83. M. Ciuchini, M. Pierini, and L. Silvestrini, “New Bounds on the CKM Matrix from $B \rightarrow K \pi$ Dalitz Plot Analyses,” Phys. Rev. D **74**, 051301 (2006).
84. M. Bona *et al.*, [UTfit Collaboration], M. Bona *et al.*, [UTfit Collaboration], “Constraints on New Physics from the Quark Mixing Unitarity Triangle,” Phys. Rev. Lett. **97**, 151803 (2006).
85. M. Bona *et al.*, [UTfit Collaboration], “The Unitarity Triangle Fit in the Standard Model and Hadronic Parameters from Lattice QCD,” JHEP **0610**, 081 (2006).
86. B. Aubert *et al.* [BABAR Collaboration], “Observation of the exclusive reaction $e^+ e^- \rightarrow \Phi \eta$ at $s^{*1/2} = 10.58$ -GeV,” Phys. Rev. D **74**, 111103 (2006).
87. B. Aubert *et al.* [BABAR Collaboration], “A structure at 2175-MeV in $e^+ e^- \rightarrow \Phi f_0(980)$ observed via initial-state radiation,” Phys. Rev. D **74**, 091103 (2006).

88. B. Aubert *et al.* [BABAR Collaboration], “Measurement of the absolute branching fractions $B \rightarrow D \pi$, $D^* \pi$, $D^{*0} \pi$ with a missing mass method,” *Phys. Rev. D* **74**, 111102 (2006).
89. B. Aubert *et al.* [BABAR Collaboration], “Measurement of the branching fraction and time-dependent CP asymmetry in the decay $B^0 \rightarrow D^{*+} D^{*-} K^0(S)$,” *Phys. Rev. D* **74**, 091101 (2006).
90. B. Aubert *et al.* [BABAR Collaboration], “Precise branching ratio measurements of the decays $D^0 \rightarrow \pi^- \pi^+ \pi^0$ and $D^0 \rightarrow K^- K^+ \pi^0$,” *Phys. Rev. D* **74**, 091102 (2006).
91. B. Aubert *et al.* [BABAR Collaboration], “Branching fraction measurements of charged B decays to $K^{*+} K^+ K^-$, $K^{*+} \pi^+ K^-$, $K^{*+} K^+ \pi^-$ and $K^{*+} \pi^+ \pi^-$ final states,” *Phys. Rev. D* **74**, 051104 (2006).
92. B. Aubert *et al.* [BABAR Collaboration], “Measurement of the ratio $B(B^+ \rightarrow X e \nu)/B(B^0 \rightarrow X e \nu)$,” *Phys. Rev. D* **74**, 091105 (2006).
93. B. Aubert *et al.* [BABAR Collaboration], “Observation of $B^+ \rightarrow \Phi \Phi K^+$ and evidence for $B^0 \rightarrow \Phi \Phi K^0$ below η/c threshold,” *Phys. Rev. Lett.* **97**, 261803 (2006).
94. B. Aubert *et al.* [BABAR Collaboration], “Observation of an excited charm baryon Ω_c^* decaying to $\Omega_c^0 \gamma$,” *Phys. Rev. Lett.* **97**, 232001 (2006).
95. B. Aubert *et al.* [BABAR Collaboration], “Observation of $B^+ \rightarrow \text{anti-}K^0 K^+$ and $B^0 \rightarrow K^0 \text{anti-}K^0$,” *Phys. Rev. Lett.* **97**, 171805 (2006).
96. B. Aubert *et al.* [BABAR Collaboration], “Search for D^0 anti- D^0 mixing and branching-ratio measurement in the decay $D^0 \rightarrow K^+ \pi^- \pi^0$,” *Phys. Rev. Lett.* **97**, 221803 (2006).
97. B. Aubert *et al.* [BABAR Collaboration], “Measurement of branching fractions and charge asymmetries in B decays to an eta meson and a K^* meson,” *Phys. Rev. Lett.* **97**, 201802 (2006).
98. B. Aubert *et al.* [BABAR Collaboration], “Measurements of branching fraction, polarization, and charge asymmetry of $B^{+-} \rightarrow \rho^{+-} \rho^0$ and a search for $B^{+-} \rightarrow \rho^{+-} f_0(980)$,” *Phys. Rev. Lett.* **97**, 261801 (2006).
99. B. Aubert *et al.* [BABAR Collaboration], “Measurement of the $B \rightarrow \pi l \nu$ branching fraction and determination of $|V_{ub}|$ with tagged B mesons,” *Phys. Rev. Lett.* **97**, 211801 (2006).
100. B. Aubert *et al.* [BaBar Collaboration], “Measurement of the branching fraction and photon energy moments of $B \rightarrow X/s \gamma$ and $A(\text{CP})(B \rightarrow X(s+d) \gamma)$,” *Phys. Rev. Lett.* **97**, 171803 (2006).
101. B. Aubert *et al.* [BABAR Collaboration], “Measurements of branching fractions, polarizations, and direct CP-violation asymmetries in $B \rightarrow \rho K^*$ and $B \rightarrow f_0(980) K^*$ decays,” *Phys. Rev. Lett.* **97**, 201801 (2006).
102. B. Aubert *et al.* [BABAR Collaboration], “Search for $B^+ \rightarrow X(3872) K^+$, $X(3872) \rightarrow J/\psi \gamma$,” *Phys. Rev. D* **74**, 071101 (2006).
103. B. Aubert *et al.* [BABAR Collaboration], “Measurements of the decays $B^0 \rightarrow \text{anti-}D^0 p \text{ anti-}p$, $B^0 \rightarrow \text{anti-}D^{*0} p \text{ anti-}p$, $B^0 \rightarrow D^- p \text{ anti-}p \pi^+$, and $B^0 \rightarrow D^{*-} p \text{ anti-}p \pi^+$,” *Phys. Rev. D* **74**, 051101 (2006).
104. B. Aubert *et al.* [BABAR Collaboration], “Observation of $e^+ e^-$ annihilations into the $C = +1$ hadronic final states $\rho^0 \rho^0$ and $\Phi \rho^0$,” *Phys. Rev. Lett.* **97**, 112002 (2006).
105. B. Aubert *et al.* [BABAR Collaboration], “Search for the decay of a B^0 or anti- B^0 meson to anti- $K^{*0} K^0$ or $K^{*0} \text{anti-}K^0$,” *Phys. Rev. D* **74**, 072008 (2006).
106. B. Aubert *et al.* [BABAR Collaboration], “Measurement of the spin of the Omega- hyperon at BABAR,” *Phys. Rev. Lett.* **97**, 112001 (2006).

107. B. Aubert *et al.* [BABAR Collaboration], “Search for the decay $B^0 \rightarrow K^0(S) K^0(S) K^0(L)$,” *Phys. Rev. D* **74**, 032005 (2006).
108. B. Aubert *et al.* [BABAR Collaboration], “Search for doubly charmed baryons Ξ/cc^+ and Ξ/cc^{++} in BABAR,” *Phys. Rev. D* **74**, 011103 (2006).
109. B. Aubert *et al.* [BABAR Collaboration], “Measurement of the $D^+ \rightarrow \pi^+ \pi^0$ and $D^+ \rightarrow K^+ \pi^0$ branching fractions,” *Phys. Rev. D* **74**, 011107 (2006).
110. B. Aubert *et al.* [BABAR Collaboration], “Search for $B^+ \rightarrow \Phi \pi^+$ and $B^0 \rightarrow \Phi \pi^0$ decays,” *Phys. Rev. D* **74**, 011102 (2006).
111. B. Aubert *et al.* [BABAR Collaboration], “Study of $B \rightarrow D^{(*)} D_{s(J)}^{(*)}$ decays and measurement of D_s^- and $D_{sJ}(2460)^-$ branching fractions,” *Phys. Rev. D* **74**, 031103 (2006).
112. B. Aubert *et al.* [BaBar Collaboration], “Search for the decay $B^0 \rightarrow a_1^+ \rho^-$,” *Phys. Rev. D* **74**, 031104 (2006).
113. B. Aubert *et al.* [BABAR Collaboration], “Measurement of the eta and eta’ transition form factors at $q^2 = 112 \text{ GeV}^2$,” *Phys. Rev. D* **74**, 012002 (2006).
114. B. Aubert *et al.* [BABAR Collaboration], “B meson decays to ωK^* , $\omega \rho$, $\omega \omega$, $\omega \phi$, and ωf_0 ,” *Phys. Rev. D* **74**, 051102 (2006).
115. B. Aubert *et al.* [BaBar Collaboration], “Search for B meson decays to eta’ eta’ K,” *Phys. Rev. D* **74**, 031105 (2006).
116. B. Aubert *et al.* [BABAR Collaboration], “Dalitz plot analysis of the decay $B^{+-} \rightarrow K^{+-} K^{+-} K^{+-}$,” *Phys. Rev. D* **74**, 032003 (2006).
117. B. Aubert *et al.* [BABAR Collaboration], “Measurement of branching fractions and CP-violating charge asymmetries for B meson decays to $D^{(*)}$ anti- $D^{(*)}$, and implications for the CKM angle gamma,” *Phys. Rev. D* **73**, 112004 (2006).
118. B. Aubert *et al.* [BABAR Collaboration], “Observation of Upsilon(4S) decays to $\pi^+ \pi^-$ Upsilon(1S) and $\pi^+ \pi^-$ Upsilon(2S),” *Phys. Rev. Lett.* **96**, 232001 (2006).
119. B. Aubert *et al.* [BABAR Collaboration], “A study of the $D/sJ^*(2317)^+$ and $D/sJ(2460)^+$ mesons in inclusive c anti-c production near $s^{*(1/2)} = 10.6\text{-GeV}$,” *Phys. Rev. D* **74**, 032007 (2006).
120. B. Aubert *et al.* [BaBar Collaboration], “Measurement of the $B^- \rightarrow D^0 K^{*-}$ branching fraction,” *Phys. Rev. D* **73**, 111104 (2006).
121. B. Aubert *et al.* [BABAR Collaboration], “Measurement of anti- $B^0 \rightarrow D^{(*)0}$ anti- $K^{(*)0}$ branching fractions,” *Phys. Rev. D* **74**, 031101 (2006).
122. B. Aubert *et al.* [BABAR Collaboration], “Search for the decay $\tau^- \rightarrow 3\pi^- 2\pi^+ 2\pi^0 \nu/\tau$,” *Phys. Rev. D* **73**, 112003 (2006).
123. B. Aubert *et al.* [BABAR Collaboration], “Study of the decay anti- $B^0 \rightarrow D^{*+} \omega \pi^-$,” *Phys. Rev. D* **74**, 012001 (2006).
124. B. Aubert *et al.* [BABAR Collaboration], “Measurements of branching fractions, rate asymmetries, and angular distributions in the rare decays $B \rightarrow K l^+ l^-$ and $B \rightarrow K^* l^+ l^-$,” *Phys. Rev. D* **73**, 092001 (2006).
125. B. Aubert *et al.* [BABAR Collaboration], “Search for the charmed pentaquark candidate Theta/c(3100)0 in $e^+ e^-$ annihilations at $s^{*(1/2)} = 10.58\text{-GeV}$,” *Phys. Rev. D* **73**, 091101 (2006).
126. B. Aubert *et al.* [BABAR Collaboration], “Measurement of branching fractions in radiative B decays to eta K gamma and search for B decays to eta’ K gamma,” *Phys. Rev. D* **74**, 031102 (2006).

127. B. Aubert *et al.* [BABAR Collaboration], “Observation of a charmed baryon decaying to $D^0 p$ at a mass near $2.94 \text{ GeV}/c^2$,” *Phys. Rev. Lett.* **98**, 012001 (2007).
128. B. Aubert *et al.* [BABAR Collaboration], “Search for T, CP and CPT violation in B^0 anti- B^0 mixing with inclusive dilepton events,” *Phys. Rev. Lett.* **96**, 251802 (2006).
129. B. Aubert *et al.* [BABAR Collaboration], “Observation of B^0 meson decay to $a_1(1260)^+ \pi^-$,” *Phys. Rev. Lett.* **97**, 051802 (2006).
130. B. Aubert *et al.* [BABAR Collaboration], “Measurements of CP-violating asymmetries and branching fractions in B decays to omega K and omega pi,” *Phys. Rev. D* **74**, 011106 (2006).
131. B. Aubert *et al.* [BABAR Collaboration], “Branching fraction limits for B^0 decays to eta’ eta, eta’ pi0 and eta pi0,” *Phys. Rev. D* **73**, 071102 (2006).
132. B. Aubert *et al.* [BaBar Collaboration], “Measurements of the branching fraction and time-dependent CP asymmetries of $B^0 \rightarrow J/\psi \pi^0$ decays,” *Phys. Rev. D* **74**, 011101 (2006).
133. B. Aubert *et al.* [BABAR Collaboration], “Measurement of time-dependent CP asymmetries in $B^0 \rightarrow D^{(*)+} \pi^-$ and $B^0 \rightarrow D^{*-} \rho^+$ decays,” *Phys. Rev. D* **73**, 111101 (2006).
134. B. Aubert *et al.* [BABAR Collaboration], “Measurements of the $B \rightarrow D^*$ form factors using the decay anti- $B^0 \rightarrow D^{*+} e^- \text{ anti-}\nu_e$,” *Phys. Rev. D* **74**, 092004 (2006).
135. B. Aubert *et al.* [BABAR Collaboration], “Determinations of $-V_{ub}$ from inclusive semileptonic B decays with reduced model dependence,” *Phys. Rev. Lett.* **96**, 221801 (2006).
136. B. Aubert *et al.* [BABAR Collaboration], “Search for the rare decays $B^0 \rightarrow D/s^{(*)+} a_0(2)^-$,” *Phys. Rev. D* **73**, 071103 (2006).
137. B. Aubert *et al.* [BABAR Collaboration], “A search for the rare decay $B^0 \rightarrow \tau^+ \tau^-$ at BABAR,” *Phys. Rev. Lett.* **96**, 241802 (2006).

Conference Presentations 2008-2005

1. Contributed Talk: K. Flood “Radiative Penguin Decays at the BaBar Experiment”, PHENO 2008, May 2008, Madison, WI.
2. Invited Talk: M. Pierini “Probing New Physics with B Decays”, Wisconsin Seminar, April 2006.
3. Invited Talk: M. Pierini “Bounds on New Physics from the Unitarity Triangle Fit”, 14th International Conference on Supersymmetry and the Unification of Fundamental Interactions”, June 2006, Irvine CA.
4. Contributed Talk: M. Pierini “Update on Charm Penguins”, CKM Workshop, Dec. 2006, Nagoya, Japan.
5. Contributed Talk: M. Pierini “CKM Fits at ILC Inspired Super Flavor Factory”, CKM Workshop, Dec. 2006, Nagoya, Japan.
6. Invited Talk: M. Pierini “Search for New Physics at a B Factory”, SLAC Seminar, Feb. 2006.
7. Invited Talk: K. Flood “Charm mixing and CP Violation Searches at BaBar”, Joint Meeting of Pacific Region Particle Physics Communities, November 2006, Honolulu, Hawaii.
8. Invited Talk: K. Flood “Recent Results in Charm Physics at Babar: Evidence for Charm Mixing”, Rencontres de Moriond, March 2007, La Thuile, Italy.
9. Contributed Talk: H. Band “Aging Studies of 2nd Generation BaBar RPCs” 2006 IEEE Nuclear Science Symposium, San Diego, California, Nov., 2006.

10. Invited Talk: H. Band "Hadronic Charm Decays" Beauty2006, Oxford, England, Sept., 2006.
11. Invited Talk: H. Band "RPC Muon Option for SiD" ALCPG Vancouver Meeting, Vancouver, Canada, June, 2006.
12. Contributed Talk: H. Band "SiD Muon System" SiD SLAC Workshop, Stanford, California, Oct., 2006.
13. Contributed Talk: H. Band "Muon Plans" SiD Fermilab Workshop, Batavia, Illinois, Dec., 2005.
14. Contributed Talk: J. Hollar, "Search for New Physics in Rare B Decays at BaBar", Pheno 06, Madison WI, May 15-17, 2006.
15. Invited Talk: M. Pierini, "Searching for new physics at a B-factory: Why, Where and How", SLAC experimental seminar, Feb. 14, 2006.
16. Invited Talk: H. Band, "Performance and Ageing Studies of BaBar Resistive Plate Chambers and Related Detectors", VIIIth Workshop on Resistive Plate Chambers and Related Detectors, Seoul, Korea Oct. 10-12, 2005.
17. Invited Talk: M. Pierini, "Unitary Triangle Fits and B Physics in the LHC/superB Era", University of Wisconsin High Energy Seminar, Madison WI. Apr. 25, 2006.
18. Invited Talk: M. Pierini, "Charming penguins model and bounds on new physics from $b \rightarrow s$ decays", SLAC experimental seminar, Sept. 1, 2005.
19. Invited Talk: M. Pierini, "Testing Standard Model and New Physics with the Unitarity Triangle Fit", PANIC 2005 Conference, Santa Fe (NM), Oct. 27, 2005.
20. Invited Talk: M. Pierini, "Rare Charmless Decays and Measurements of alpha and beta in Penguins", Flavor in the era of the LHC" workshop, CERN Geneva, Nov. 8, 2005.
21. Invited Talk: M. Pierini, "Impact of energy spread on New Physics probes", First SuperB workshop, Frascati (Italy), Nov. 11, 2005.
22. Invited Talk: M. Pierini, "Status and Perspectives of the BaBar experiment", Experimental seminar LAL, Orsay (France), Nov. 20, 2005.
23. Invited Talk: M. Pierini, "Impact of B physics in New Physics search with the BaBar detector", Experimental seminar Univ. Roma "La Sapienza", Rome (Italy), Nov. 28, 2005.
24. Contributed Talk: J. Hollar, "Electroweak Penguin Decays at BaBar", Frontiers in Contemporary Physics - III, Nashville, TN. May 2005.
25. Contributed Talk: J. Hollar, "B Factory Measurements of $b \rightarrow sll$ and Prospects for $b \rightarrow dll$ ", CKM2005 Workshop, La Jolla, California, March 15-18, 2005.
26. Invited Talk: S. Dasu, "Radiative Penguin Decays of B Mesons", CERN Seminar, July 11, 2005.
27. Invited Talk: S. Dasu, "Search for New Physics at B-Factories" The 12th International Conference on Supersymmetry and Unification of Fundamental Interactions, Tsukuba, Japan, June, 2004
28. Contributed Talk: H. R. Band, "Performance of 2nd Generation RPCs in BaBar", 2004IEEE, Nuclear Science Symposium, Rome, Italy, Oct. 2004.
29. Contributed Talk: K. Flood, "Review of Charm Mixing", HQL 2004, San Juan, Puerto Rico, June, 2004.
30. Contributed Talk: A. Eichenbaum, "Measurement of the Direct CP Asymmetry in $b \rightarrow s\gamma$ Decays", APS Meeting, Denver, May 2004.

31. Contributed Talk: P. Tan, “Measurement of Branching Fractions, CP Asymmetry, and Isospin Asymmetry of $B \rightarrow K^* \gamma$ Decays”, APS Meeting, Denver, May 2004.
32. Contributed Talk: J. Hollar, “Observation of the Rare Decays $B \rightarrow K^* l^+ l^-$ and $B \rightarrow K l^+ l^-$ ”, APS Meeting, Denver, May 2004.